MOLECULAR AND CELLULAR BIOLOGY, June 2002, p. 3905–3926 Vol. 22, No. 11
0270-7306/02/$04.00+0 DOI: 10.1128/MCB.22.11.3905–3926.2002

Intracellular Retention of Glycosylphosphatidyl Inositol-Linked Proteins in Caveolin-Deficient Cells

Federica Sotgia,[1,2] Babak Razani,[1] Gloria Bonuccelli,[1,2] William Schubert,[1] Michela Battista,[1] Hyangkyu Lee,[1] Franco Capozza,[1] Ann Lane Schubert,[1] Carlo Minetti,[2] J. Thomas Buckley,[3] and Michael P. Lisanti[1,4]*

Department of Molecular Pharmacology[1] and Division of Hormone-Dependent Tumor Biology,[4] The Albert Einstein Comprehensive Cancer Center, Albert Einstein College of Medicine, Bronx, New York 10461; Servizio Malattie Neuro-Muscolari, Università di Genova, Istituto Gaslini, 16147 Genoa, Italy[2]; and Department of Biochemistry and Microbiology, University of Victoria, Victoria, British Columbia V8W 3P6, Canada[3]

Received 14 December 2001/Returned for modification 12 February 2002/Accepted 26 February 2002

The relationship between glycosylphosphatidyl inositol (GPI)-linked proteins and caveolins remains controversial. Here, we derived fibroblasts from Cav-1 null mouse embryos to study the behavior of GPI-linked proteins in the absence of caveolins. These cells lack morphological caveolae, do not express caveolin-1, and show a ~95% down-regulation in caveolin-2 expression; these cells also do not express caveolin-3, a muscle-specific caveolin family member. As such, these caveolin-deficient cells represent an ideal tool to study the role of caveolins in GPI-linked protein sorting. We show that in Cav-1 null cells GPI-linked proteins are preferentially retained in an intracellular compartment that we identify as the Golgi complex. This intracellular pool of GPI-linked proteins is not degraded and remains associated with intracellular lipid rafts as judged by its Triton insolubility. In contrast, GPI-linked proteins are transported to the plasma membrane in wild-type cells, as expected. Furthermore, recombinant expression of caveolin-1 or caveolin-3, but not caveolin-2, in Cav-1 null cells complements this phenotype and restores the cell surface expression of GPI-linked proteins. This is perhaps surprising, as GPI-linked proteins are confined to the exoplasmic leaflet of the membrane, while caveolins are cytoplasmically oriented membrane proteins. As caveolin-1 normally undergoes palmitoylation on three cysteine residues (133, 143, and 156), we speculated that palmitoylation might mechanistically couple caveolin-1 to GPI-linked proteins. In support of this hypothesis, we show that palmitoylation of caveolin-1 on residues 143 and 156, but not residue 133, is required to restore cell surface expression of GPI-linked proteins in this complementation assay. We also show that another lipid raft-associated protein, c-Src, is retained intracellularly in Cav-1 null cells. Thus, Golgi-associated caveolins and caveola-like vesicles could represent part of the transport machinery that is necessary for efficiently moving lipid rafts and their associated proteins from the trans-Golgi to the plasma membrane. In further support of these findings, GPI-linked proteins were also retained intracellularly in tissue samples derived from Cav-1 null mice (i.e., lung endothelial and renal epithelial cells) and Cav-3 null mice (skeletal muscle fibers).

Over the past 10 years, increasing evidence has suggested that the plasma membrane is not a homogenous "sea of lipids" in which the proteins freely diffuse but instead is composed of distinct membrane microdomains characterized by the local accumulation of different lipids and proteins (29). In particular, recent studies support the existence of cholesterol- and sphingolipid-rich membrane domains, which have been termed lipid rafts (29, 87).

The close packing of cholesterol and sphingolipids makes these microdomains more ordered and less fluid than the rest of the bulk plasma membrane and confers upon these membrane domains special biophysical properties, making them resistant to solubilization with nonionic detergents at low temperatures (1, 6, 9). Moreover, the existence of lipid rafts helps to regulate the lateral diffusion of proteins and dictates energetic rules so that the segregation of lipid-modified proteins (either exoplasmic GPI-linked proteins or cytoplasmically oriented acylated proteins, such as Src-family kinases) is favored (8).

These lipid raft domains can exist by themselves or can be enriched in one particular structural protein which can dramatically modify their form and function (29). The first integral membrane protein identified as a lipid raft modifier was caveolin (52, 75, 78); when the caveolin protein is integrated into the microenvironment of a lipid raft, a caveolar vesicle is generated (29, 42). As a consequence, several discrete classes of microdomains exist within the plane of the plasma membrane, i.e., non-caveolar lipid rafts and caveolar lipid rafts, among others (29, 87). Lipid rafts are localized mainly at the level of the plasma membrane, but they can also form within internal membrane compartments, such as the Golgi (31). Therefore, the partitioning of caveolins into these lipid raft domains may begin to occur at the level of the Golgi apparatus (31), initiating the biogenesis of caveolae.

Caveolin is only the first of a three-member gene family, and as a consequence, caveolin has been retermed caveolin-1 (82, 92). Caveolin-1 and -2 are coexpressed and show nearly identical tissue distributions, whereas caveolin-3 is expressed in a muscle-specific fashion (70, 82, 89, 92). As a result of its cho-

* Corresponding author. Mailing address: Department of Molecular Pharmacology, The Albert Einstein Cancer Center, Albert Einstein College of Medicine, 1300 Morris Park Ave., Bronx, NY 10461. Phone: (718) 430-8828. Fax: (718) 430-8830. E-mail: lisanti@aecom.yu.edu.

lesterol-binding activity (43, 61, 94), caveolin-1 is thought to play a central role in the formation of plasmalemmal caveolae, morphologically defined as 50- to 100-nm diameter invaginations of the plasma membrane.

In the process of the formation of caveolae, caveolin-1 and caveolin-2 hetero-oligomerize to form high-molecular-mass structures (15, 57, 77, 81). The interaction of these caveolin oligomers with cholesterol and sphingolipids may play a critical role at this stage by inducing the clustering and recruitment of certain lipid-modified membrane proteins while excluding other transmembrane proteins and lipid components (52, 87).

Caveolae were first independently described by two pioneers in the field of electron microscopy, Yamada and Palade, in the early 1950s (66, 95). Omega-shaped invaginations occurring singly or in clusters, caveolae are found in many different cell types, but are most abundant in fibroblasts, adipocytes, endothelial cells, type I pneumocytes, epithelial cells, and smooth muscle cells. Although they were first described as endocytic structure for the transport of both small and large molecules across endothelial cells (86), they are now considered a complex membrane system that participates in many cellular functions. Most notably, caveolae are dramatically enriched in lipid-modified cytoplasmic signaling molecules, including Src family tyrosine kinases, heterotrimeric G proteins, and nitric oxide synthase, among others (14, 52). As a consequence, caveolae are believed to act as message centers that coordinate signal transduction processes at the plasma membrane (52, 87).

Over the last decade, much attention has been focused on a class of proteins which are attached to the external surface of the plasma membrane through a C-terminal lipid moiety, termed glycosylphosphatidyl inositol (GPI). In polarized epithelial cells, GPI-linked proteins are selectively transported to the apical surface through the exocytic pathway while preferentially excluded from the basolateral membrane (7, 44, 47, 49, 51, 91). The GPI-linked family of proteins shows a wide functional diversity of members that includes molecules that participate in cell-cell adhesion, cell surface interactions, and signal transduction (23, 50).

What is known about the biogenesis of GPI-anchored proteins? Although side chain modifications and the fatty acid composition of the GPI anchor may vary, all GPI anchors contain a conserved core glycan structure. Precursor proteins that are destined to be GPI anchored contain a GPI attachment signal at their extreme C terminus that is cleaved and replaced with a GPI moiety within the lumen of the ER (11, 12, 60). At the level of the trans-Golgi network, GPI-linked proteins then begin to partition into lipid raft microdomains and become resistant to solubilization by the detergent Triton X-100 (6). In this regard, it is thought that the GPI anchor acts as a targeting signal for the association of this class of proteins with lipid rafts. However, it remains unknown how GPI-anchored proteins are then transported from lipid rafts at the trans-Golgi to lipid rafts at the cell surface. It has been proposed that caveola-like vesicles located at the level of the Golgi might act as exocytic vesicular carriers to transport GPI-linked proteins to the cell surface (45, 54, 78). However, evidence to directly support this hypothesis is lacking. Thus, the exact biosynthetic functional relationship between GPI-anchored proteins, caveolae, and the caveolin proteins remains controversial.

Here, we investigate whether a loss of caveolin protein expression and caveolae directly affects the cellular distribution of GPI-anchored proteins. For this purpose, we studied the membrane trafficking of GPI-linked proteins in caveolin-deficient mouse models (28, 73). Using standard homologous recombination techniques, we recently generated caveolin-1 null mice and derived mouse embryo fibroblasts (MEFs) from these animals (72). These cells lack morphological caveolae, do not express caveolin-1, and show a ~95% down-regulation in caveolin-2 expression; these cells also do not express caveolin-3, a muscle-specific caveolin family member. As such, these caveolin-deficient cells represent the ideal tool to study the role of caveolins in GPI-linked protein sorting. In order to visualize endogenous GPI-linked proteins as a general class of molecules, we employed a lectin-like bacterial toxin, aerolysin, which selectively recognizes the core glycan structure of the GPI anchor only when it is attached to proteins (5, 16, 62). Consequently, aerolysin does not discriminate between the different GPI-anchored proteins (16). Similar experiments were carried out using skeletal muscle tissue samples derived from caveolin-3 null mice (28, 30).

We now show that expression of palmitoylated caveolin-1 is normally required for the efficient transport of GPI-linked proteins from the Golgi complex to the plasma membrane. Our current results are entirely consistent with the original identification of caveolin-1 as VIP-21 (vesicular integral membrane protein with a molecular mass of 21 kDa), a prominent component of trans-Golgi-derived transport vesicles (reviewed in references 29, 52, and 73).

MATERIALS AND METHODS

Materials. Antibodies and their sources were as follows: anti-caveolin-1 monoclonal antibody (MAb) (clone 2297), anti-caveolin-2 MAb (clone 65), and anti-caveolin-3 MAb (clone 26) (81, 83, 89) (gifts of Roberto Campos-Gonzalez, BD Transduction Laboratories, Inc.); anti-caveolin-1 poloclonal antibody (PAb) N-20 (Santa Cruz Biotechnology); anti-caveolin-2 PAb and anti-caveolin-3 PAb (Affinity Bioreagents, Inc.); anti-β-dystroglycan (mouse MAb; Novocastra); anti-Cab45 PAb (gift of Philipp E. Scherer); proaerolysin and anti-aerolysin MAb (Protox Biotech); anti-aerolysin rabbit PAb (16, 62) (Buckley laboratory); anti-T-cadherin PAb H-126 (Santa Cruz Biotechnology); anti-Tamm-Horsfall glycoprotein sheep PAb (Chemicon, Inc.); anti-Src MAb (Upstate Biotechnology); anti-β-actin MAb (clone AC-15) (Sigma); anti-carbonic anhydrase-IV PAb (CA-IV; gift of William S. Sly, St. Louis University School of Medicine). A variety of other reagents were purchased commercially as follows: cell culture reagents and the Lipofectamine liposomal transfection reagent were from Gibco/BRL.

Expression vectors. The cDNAs encoding full-length caveolin-1, caveolin-2, and caveolin-3 were subcloned into pCB7, a mammalian expression vector driven by the cytomegalovirus promoter (15, 81–83, 92). The cDNAs encoding the wild-type caveolin-1 and the caveolin-1 palmitoylation mutants (17) were not epitope tagged and were subcloned into the pCAGGS vector, as we previously described (38, 39). The cDNA encoding human c-Src in the pUSE-Amp cytomegalovirus-based vector was purchased from Upstate Biotechnology, Inc.

Immunoblot analysis. Mouse tissues were harvested, minced with a scissors, homogenized in a Polytron tissue grinder for 30 s at a medium-range speed, and solubilized with lysis buffer (10 mM Tris, pH 8; 150 mM NaCl; 1% Triton X-100, 60 mM octyl glucoside) containing protease inhibitors (Boehringer Mannheim). In order to prepare cell lysates, cells were cultured in their respective media and allowed to reach ~80 to 90% confluency. Subsequently, they were washed with phosphate-buffered saline (PBS) and incubated with lysis buffer containing protease inhibitors. Protein concentrations were quantified using the bicinchoninic acid reagent (Pierce), and the volume required for 10 μg of protein was determined. Samples were separated by sodium dodecyl sulfate-polyacrylamide gel electrophoresis (SDS-PAGE) (10% acrylamide) and transferred to nitrocellulose. The nitrocellulose membranes were stained with Ponceau S (to visualize protein bands), followed by immunoblot analysis. All subsequent wash buffers contained 10 mM Tris (pH 8.0)–150 mM NaCl–0.05% Tween-20, which was

supplemented with 1% bovine serum albumin (BSA) and 4% nonfat dry milk (Carnation) for the blocking solution and 1% BSA for the antibody diluent. Primary antibodies were used at a 1:1,000 dilution. Horseradish peroxidase-conjugated secondary antibodies (1:5,000 dilution; Pierce) were used to visualize bound primary antibodies with the Supersignal chemiluminescence substrate (Pierce).

Proaerolysin overlay assays. GPI-linked proteins were visualized using the proaerolysin overlay assay (5, 16, 62). Briefly, samples were separated by SDS-PAGE (10% acrylamide) and transferred to nitrocellulose. Membranes were blocked with 4% lowfat dried milk and 1% BSA in PBST (PBS–0.5% Tween 20). Blots were then incubated at room temperature for 1 h with 20 nM proaerolysin in PBST, washed three times, and incubated with a 1:4,000 dilution of an anti-aerolysin MAb probe. After washing for 15 min, membranes were incubated with an anti-mouse antibody conjugated to horseradish peroxidase (Pierce). Bound immunoglobulin G (IgG) was detected using a chemiluminescent substrate (Pierce).

Purification of caveola-enriched membrane fractions. Caveola-enriched membrane fractions were purified essentially as we previously described (53, 78). Briefly, 200 mg of lung tissue was placed in 2 ml of MBS (25 mM MES [morpholineethanesulfonic acid], pH 6.5, 150 mM NaCl) containing 1% Triton X-100 and solubilized by using rapid 10-s bursts of a rotor homogenizer and passing 10 times through a loose-fitting Dounce homogenizer. The sample was mixed with an equal volume of 80% sucrose (prepared in MBS lacking Triton X-100), transferred to a 12-ml ultracentrifuge tube, and overlaid with a discontinuous sucrose gradient (4 ml of 30% sucrose, 4 ml of 5% sucrose, both prepared in MBS lacking detergent). The samples were subjected to centrifugation at 200,000 $\times g$ (39,000 rpm in a Sorval rotor TH-641) for 16 h. A light-scattering band was observed at the 5/30% sucrose interface. Twelve 1-ml fractions were collected, and 10 μg of each fraction were subjected to SDS-PAGE and either to immunoblotting or to the proaerolysin overlay assay.

Immunostaining of paraffin sections. Tissue sections derived from wild-type and Cav-1 null mice were deparaffinized in xylene for 4 min and rehydrated through a graded series of ethanol and placed in PBS. Antigen retrieval was performed by microwave irradiation in 0.01 M trisodium citrate buffer, pH 6. Sections were preblocked in PBS supplemented with 1% BSA, 10% horse serum, and 0.1% Triton X-100 for 1 h at room temperature. The sections were then labeled with a given polyclonal primary antibody at room temperature for 1 h. After a 15-min wash in PBS, rhodamine-conjugated secondary antibodies were added to the sections for 30 min. The sections were then washed in PBS for 15 min. Slow-Fade antifade reagent was added to prevent bleaching of the fluorochrome. Samples were imaged with an Olympus inverted microscope. For the nuclear counterstaining, before mounting the slides, DAPI was added for 15 min at room temperature.

3T3 MEF culture and transfection. MEFs were obtained from day 13.5 embryos and immortalized using the 3T3 protocol, as we previously described (72). Immortalized MEF cells were grown in Dulbecco minimal essential medium supplemented with 10% fetal bovine serum (FBS), 2 mM glutamine, 100 U of penicillin/ml, and 100 μg of streptomycin (Gibco/BRL)/ml. Cells (~40 to 50% confluent) were transiently transfected with a given cDNA by using the Lipofectamine liposomal transfection reagent, per the manufacturer's instructions, and analyzed 36 to 48 h posttransfection.

Immunofluorescence microscopy. The procedure was performed essentially as we have previously described, with minor modifications (40, 72). MEFs (either untransfected or transfected) were fixed for 30 min in PBS containing 2% paraformaldehyde and rinsed with PBS. The cells were then incubated in permeabilization buffer (PBS, 0.2% BSA, 0.1% Triton X-100) for 10 min, washed with PBS, and labeled with 10^{-8} M proaerolysin. After washing with PBS (three times), cells were incubated with a 1:500 dilution of an anti-aerolysin MAb. The bound primary antibody was visualized with a tagged secondary antibody (fluorescein isothiocyanate [FITC]-conjugated goat anti-mouse IgG [Jackson Immunochemicals]). Cells were then washed with PBS (three times), and slides were mounted with Slow-Fade anti-fade reagent (Molecular Probes). A cooled charge-coupled device camera attached to an Olympus microscope was used for detection of bound secondary antibodies. For double-labeling experiments, the appropriate primary polyclonal antibody was incubated along with the anti-aerolysin MAb and detected with a lissamine-rhodamine-conjugated goat anti-rabbit secondary antibody (Jackson Immunochemicals).

Biochemical detection of cell surface GPI-linked proteins. Wild-type and Cav-1 null 3T3 MEFs were grown to confluence on 10-cm-diameter dishes, washed twice with ice-cold PBS containing $CaCl_2$ (0.1 mM) and $MgCl_2$ (1 mM) [PBS-C/M], and subjected to cell surface biotinylation with sulfo–*N*-hydroxysuccinimide (NHS)–biotin (0.5 mg/ml; Pierce), essentially as we have described previously (51, 76). Then, the cells were scraped into 1 ml of ice-cold lysis buffer containing 10 mM Tris, pH 8.0, 0.15 M NaCl, 1% Triton X-114, and protease inhibitors and homogenized with a Dounce (five strokes). After 30 min on ice, the samples were briefly warmed to 37°C (for 2 to 3 min); this step allows the solubilization of GPI-linked proteins and causes the detergent Triton X-114 to undergo phase separation (45, 51). The detergent phase was collected by centrifugation in the Microfuge (14, 000 $\times g$ for 30 s) at room temperature; hydrophobic integral membrane proteins (including GPI-linked proteins) are known to partition almost exclusively into the lower Triton X-114 detergent phase (46, 49). The detergent phase (~100 to 150 μl) was then diluted with 900 μl of ice-cold 10 mM Tris, pH 8.0, 0.15 M NaCl, 60 mM octyl-glucoside, and protease inhibitors. After dilution of the detergent phase, the samples were then subjected to centrifugation in the Microfuge (14, 000 $\times g$ for 10 min) at 4°C to remove any material that was not solubilized. The resulting lysates were precleared with protein A-Sepharose. Then, streptavidin-agarose beads (50 μl of a slurry) were added to each tube to collect the biotinylated cell surface integral membrane proteins (48) (including GPI-linked proteins) and the samples were incubated for 4 to 6 h at 4°C rotating in the cold room. After washing the streptavidin-beads (three times) with ice-cold 10 mM Tris, pH 8.0, 0.15 M NaCl, 60 mM octyl-glucoside, and protease inhibitors, the bound material was eluted by boiling in SDS-PAGE sample buffer. After SDS-PAGE and transfer to nitrocellulose, GPI-linked proteins were visualized using the proaerolysin overlay assay, as described above. Two 10-cm-diameter plates of cells were used for each experimental condition.

Triton X-100 insolubility. MEFs were washed twice with ice-cold PBS; then, a buffer containing 25 mM MES, pH 6.5, 0.15 M NaCl, 1% Triton X-100, and protease inhibitors was gently added to the cells (90). After 30 min of incubation at 4°C without agitation, the soluble fraction was collected. The insoluble fraction was extracted using 1% SDS. Equal volumes of the soluble and insoluble fractions were resolved by SDS-PAGE (10% acrylamide) and analyzed by proaerolysin overlay or by immunoblotting.

Immunostaining of skeletal muscle sections. Gastrocnemius muscles were isolated from wild-type and Cav-3 null mice, rapidly frozen in liquid nitrogen-cooled isopentane, and stored in liquid nitrogen. Unfixed frozen sections (6 μm thick) of skeletal muscle were prepared and then blocked with 1% BSA, 10% horse serum, and 0.1% Triton X-100 for 1 h at room temperature. Sections were incubated with a given primary antibody diluted in PBS containing 1% BSA. After three washes with PBS, sections were incubated with the appropriate secondary antibody (FITC-conjugated goat anti-mouse antibody or lissamine-rhodamine-conjugated goat anti-rabbit antibody). Finally, the sections were washed three times with PBS and the slides were mounted with the Slow-Fade antifade reagent. For proaerolysin staining, sections were blocked as described above and labeled with 10^{-8} M proaerolysin. After washing with PBS (three times), cells were incubated with a 1:500 dilution of an anti-aerolysin rabbit PAb. The bound primary antibody was visualized with a rhodamine-conjugated anti-rabbit secondary antibody. Slides were then washed with PBS (three times) and mounted with the Slow-Fade antifade reagent.

Cholera toxin uptake studies. Wild-type and Cav-1 null 3T3 MEFs were grown on glass coverslips, and the cells were washed twice with ice-cold PBS containing $CaCl_2$ (0.1 mM) and $MgCl_2$ (1 mM) (PBS-C/M). Cholera toxin B subunit (CT-B; Sigma) was then diluted into ice-cold PBS-C/M for a final concentration of 1 μg/ml. The diluted CT-B solution was then applied to the cells. After 30 min on ice, the cells were then washed twice with ice-cold PBS-C/M and normal media (prewarmed to 37°C) was added. The cells were then incubated at 37°C for various times (5, 15, 30, and 45 min) to allow CT-B internalization. Internalization of CT-B was then stopped by placing the cells on ice, washing with ice-cold PBS-C/M (two times), and fixation with 2% para-formaldehyde. Immunofluorescent detection of the CT-B was performed using a rabbit polyclonal anti-CT-B antibody (Sigma). The bound primary antibody was visualized with a rhodamine-conjugated anti-rabbit secondary antibody.

RESULTS

In lung tissue from Cav-1-deficient mice, GPI-anchored proteins are expressed at normal levels and are correctly targeted to lipid rafts but are retained in an intracellular perinuclear compartment. In order to understand the effect of a caveolin-1 deficiency on the phenotypic behavior of GPI-linked proteins, we first analyzed lung tissue samples from Cav-1 null mice as the caveolin-1 protein is normally highly expressed in the lung, an endothelial-rich tissue source. Lysates were prepared from

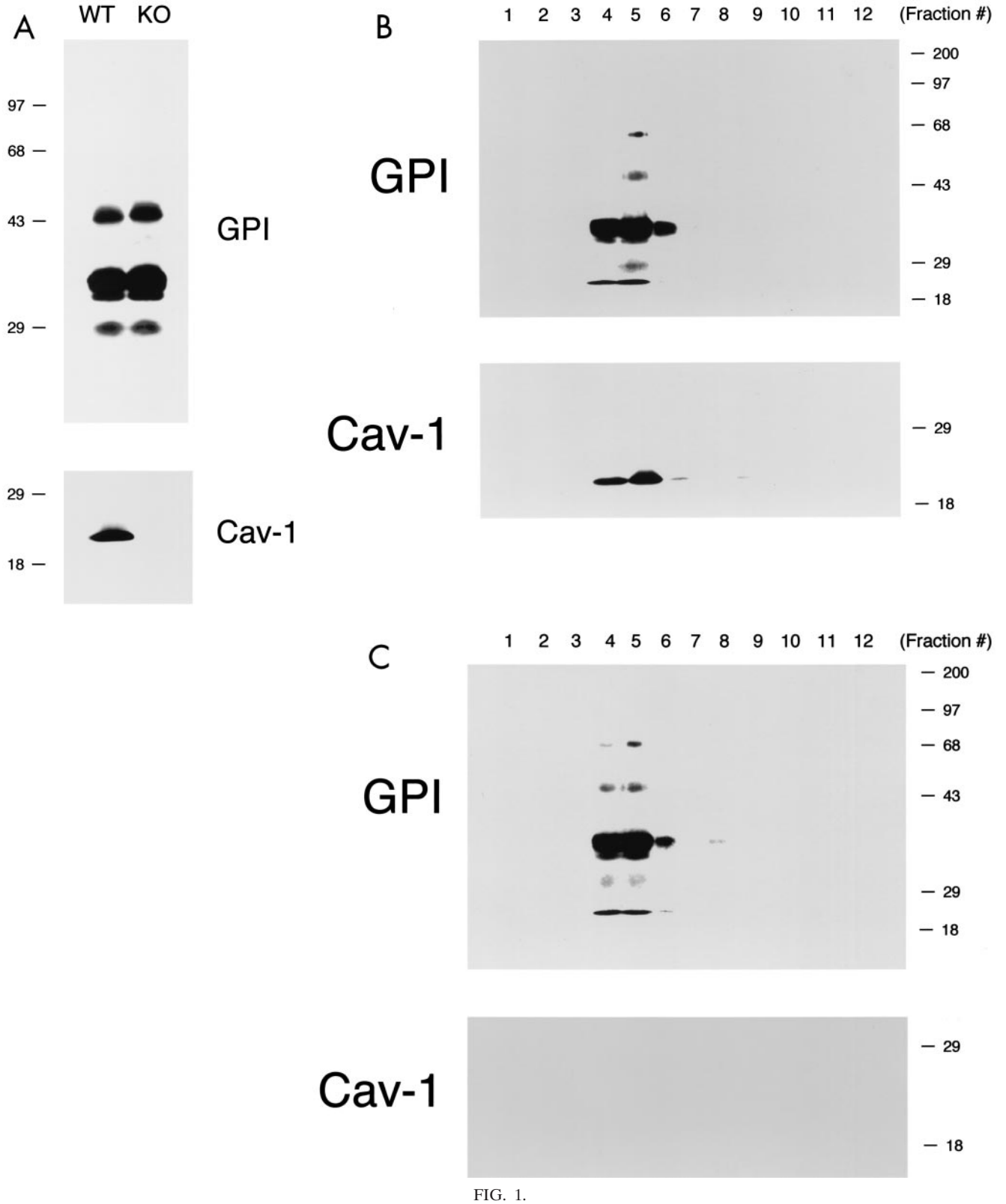

FIG. 1.

wild-type and Cav-1 null lung tissue and subjected to SDS-PAGE/proaerolysin overlay analysis. Figure 1A shows that, surprisingly, GPI-anchored proteins were expressed at normal levels in Cav-1 null mice.

Previous studies have shown that GPI-anchored proteins are normally targeted to lipid rafts which are membrane microdomains that are enriched in cholesterol and sphingolipids (1, 6). The cholesterol/sphingolipid-rich composition of lipid rafts makes them more ordered than the rest of the plasma membrane and confers upon them special biochemical properties.

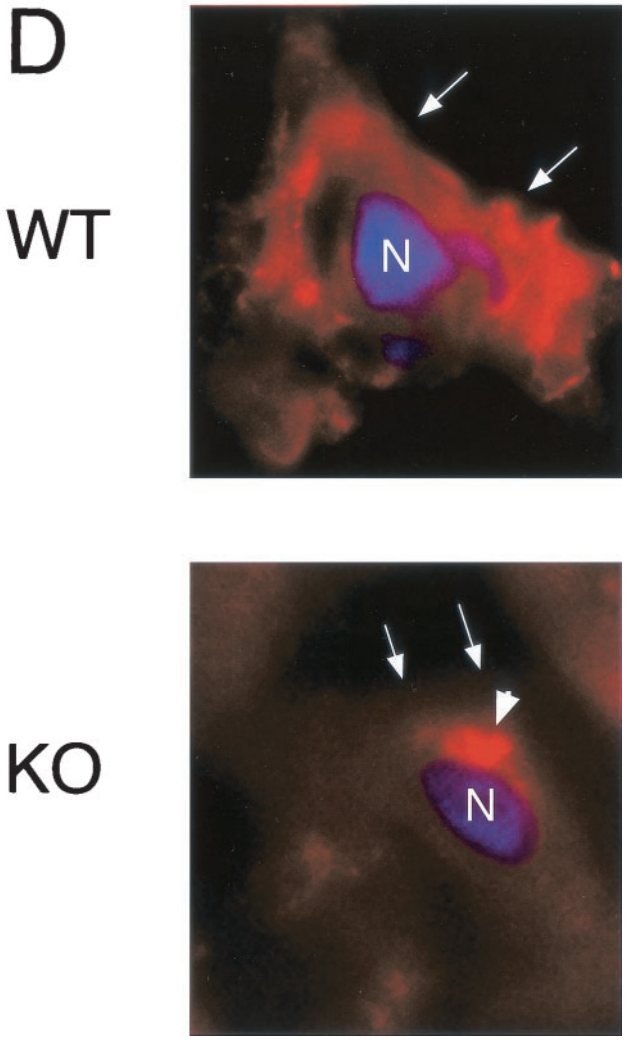

FIG. 1. Phenotypic behavior of GPI-anchored proteins in lung tissue from Cav-1 null mice. (A) GPI Western blot analysis. The expression levels of lung GPI-anchored proteins remain unchanged in Cav-1 null mice compared with those of wild-type control mice. Lung tissue samples from wild-type and Cav-1 null mice were homogenized in lysis buffer, and 20 μg of lysate from each sample was separated by SDS-PAGE. After transfer to nitrocellulose, the blots were subsequently subjected to proaerolysin overlay to visualize GPI-linked proteins or to caveolin-1 immunoblotting. (B and C) Cellular fractionation. GPI-anchored proteins were targeted to lipid rafts/caveola-enriched fractions in lung tissue from wild-type and Cav-1 null mice. Lipid rafts/caveola microdomains were separated from other cellular constituents by using sucrose flotation gradients (see Materials and Methods). Lung tissue from wild-type and Cav-1 null mice was homogenized thoroughly in lysis buffer containing 1% Triton X-100 and subjected to sucrose gradient centrifugation. Twelve 1-ml fractions were collected, and 10 μg of each fraction was separated by SDS-PAGE and transferred to nitrocellulose. The distribution of GPI-anchored proteins was analyzed by proaerolysin overlay. Note that GPI-anchored proteins cofractionate with caveolin-1 (fractions 4 and 5) in lung tissue from wild-type mice (B). However, GPI-anchored proteins are still targeted to lipid rafts (fractions 4 and 5) in lung tissue from Cav-1 null mice (C). (D) CA-IV immunostaining. GPI-linked proteins show differences in their localization patterns in lung tissue from Cav-1 null mice. Lung paraffin sections from wild-type and Cav-1 null mice were labeled with an antibody directed against an abundant lung endothelial GPI-anchored protein, CA-IV. Bound primary antibodies were detected with a fluorescently labeled secondary antibody. Nuclear counterstaining was performed using DAPI. Top, CA-IV localizes at the plasma membrane in wild-type lung endothelial cells (see arrows). Bottom, GPI-anchored CA-IV shows a perinuclear localization pattern in Cav-1 null lung endothelial cells (see arrowhead); arrows point to the cell surface.

In particular, lipid rafts are resistant to solubilization with nonionic detergents at low temperatures, thereby facilitating their purification (8, 9). When the caveolin-1 protein is expressed, it is targeted to lipid rafts, where it induces the transformation of lipid rafts into caveolar microdomains (29, 87).

To determine if GPI-anchored proteins are correctly targeted to lipid rafts in Cav-1 null mice, lung tissue samples were next subjected to extraction with ice-cold Triton X-100 and sucrose density gradient ultracentrifugation, an established procedure that allows the purification of lipid rafts/caveolae (53, 55, 78, 90); fractions 4 and 5 contained caveolin-1 and represented the lipid raft/caveola-enriched fractions, while fractions 8 to 12 contained the bulk of cellular membranes and cytosolic proteins. To visualize the distribution of GPI-linked proteins across the gradient, an aliquot of each gradient fraction was subjected to SDS-PAGE and proaerolysin overlay analysis. Figure 1B and C shows that GPI-linked proteins are correctly targeted to lipid rafts in Cav-1 null mice (Fig. 1C), compared to normal wild-type controls (Fig. 1B). These results indicate that caveolin-1 expression is clearly not required for maintaining the association of GPI-linked proteins with lipid rafts.

We next investigated the subcellular localization of GPI-anchored proteins. For this purpose, we immunostained lung paraffin sections from wild-type and Cav-1 null mice with rabbit PAbs directed against carbonic anhydrase IV (CA-IV). CA-IV is a GPI-linked enzyme originally purified from lung tissue, and CA-IV is prominently expressed on the luminal side of the alveolar capillary endothelium (24). Samples were also subjected to nuclear counterstaining with DAPI (4,6-diamidino-2-phenylindole), which emits blue fluorescence upon binding to AT-rich DNA regions.

Figure 1D shows that in wild-type mice, CA-IV was expressed on the plasma membrane, as expected. In striking contrast, CA-IV was retained in an intracellular perinuclear compartment in Cav-1 null mice. Thus, the trafficking of lipid rafts/GPI-linked proteins may be altered in Cav-1 null mice.

Intracellular retention of GPI-linked proteins within lipid rafts at the Golgi complex in Cav-1-deficient 3T3 MEFs. To better understand the altered localization of GPI-linked proteins in lung tissue samples, we next analyzed the behavior of GPI-linked proteins in MEFs derived from Cav-$1^{+/+}$ and Cav-$1^{-/-}$ animals (72). These cells constitute an ideal model for studying how caveolin-1 may affect the trafficking of various endogenously expressed proteins, such as GPI-anchored proteins, under physiological conditions.

Two different MEF clones for each genotype (wild-type and Cav-1 null) were generated in our laboratory and immortalized using a defined 3T3-passaging protocol (72). Here, we present the first characterization of these 3T3-immortalized wild-type and Cav-1 null MEF clones. These four new cell lines (>35 passages) will be extremely useful in studying the role of caveolae and caveolin-1 in membrane protein trafficking, as they provide a highly transfectable mammalian complementation system for studying caveolin-1-dependent cell function(s). Immunoblot analysis of protein lysates from wild-type and Cav-1 null 3T3 MEFs revealed a complete absence of caveolin-1 expression and a dramatic reduction of caveolin-2 expression in Cav-1 null 3T3 MEFs (Fig. 2A). These findings are consistent with our previous results using primary cultures of wild-type and Cav-1 null MEFs (passages 1 to 5) (72). Equal protein loading was assessed by immunoblotting with anti-β-actin IgG.

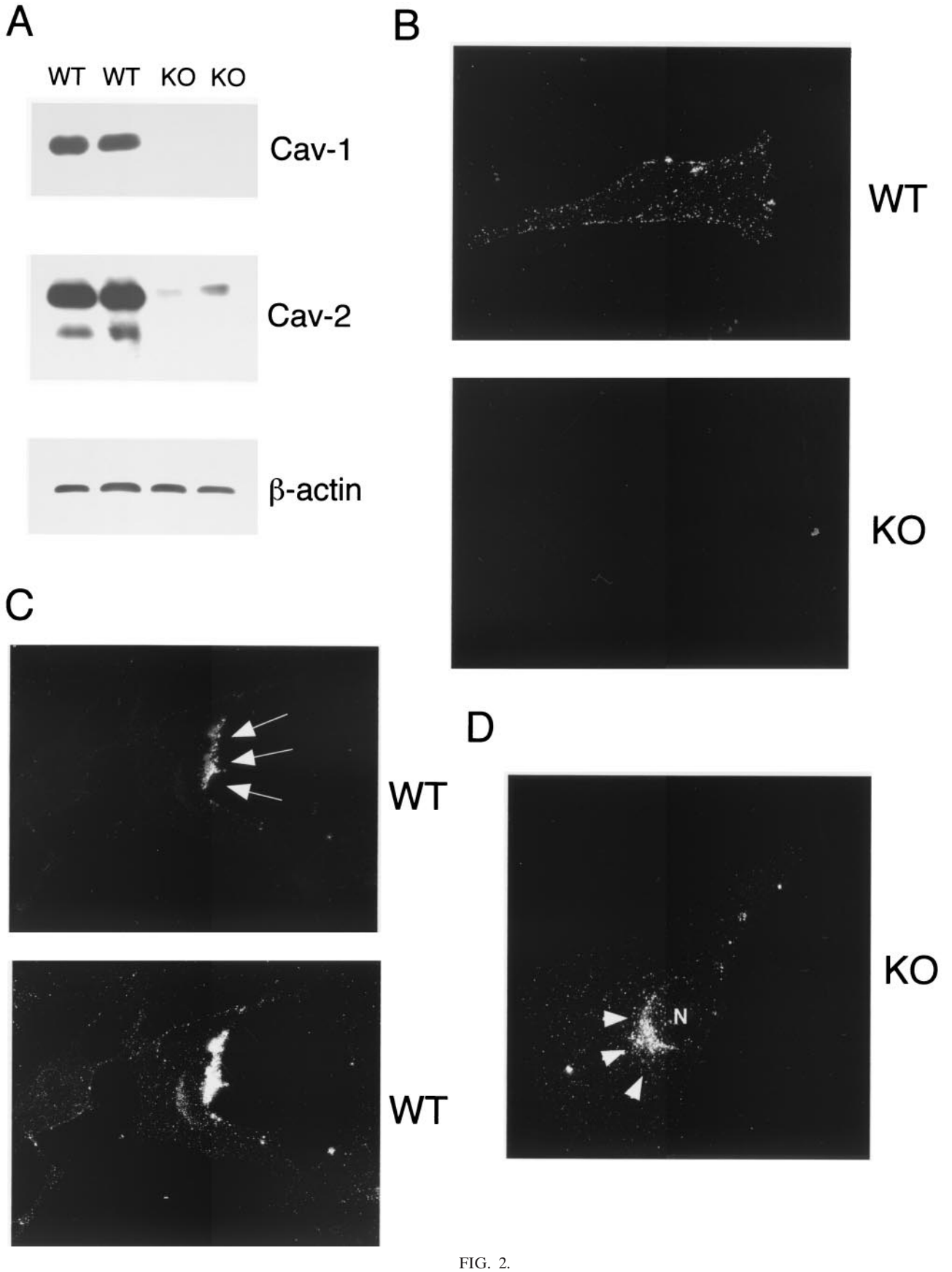

FIG. 2.

We first assessed the localization of GPI-linked proteins by cell surface staining using wild-type and Cav-1 null MEFs. Cells were fixed in the absence of any detergents and subjected to labeling with proaerolysin. Figure 2B (lower panel) shows that little or no GPI surface staining was detectable in Cav-1 null cells. On the contrary, in wild-type MEFs, GPI-anchored proteins showed their normal characteristic punctate distribution at the cell surface (Fig. 2B, upper panel). Identical results were obtained with both Cav-1 null 3T3 MEF clones.

We next performed immunolocalization after permeabilization with detergent to allow the detection of a potential intracellular pool of GPI-linked proteins with proaerolysin. In wild-type MEFs, GPI-linked proteins were efficiently targeted to the plasma membrane, and in fact, they often showed a polarized distribution; two exposures are shown to better illustrate this point (Fig. 2C). However, in Cav-1 null MEFs, GPI-linked proteins were primarily retained at the level of a perinuclear compartment and were not able to efficiently reach the plasma membrane (Fig. 2D). This finding is consistent with the observed intracellular retention of GPI-linked proteins in the lung tissue samples (Fig. 1D). We identified this perinuclear compartment as the Golgi complex (Fig. 3A) by performing double-labeling experiments with antibodies directed against a Golgi marker protein, Cab45, that is endogenously expressed (80).

Given the observed intracellular retention of GPI-linked proteins, we wondered if such localization might affect their stability or their expression levels. To our surprise, however, GPI-anchored proteins were expressed at normal levels in Cav-1 null MEFs, as seen by proaerolysin overlay (Fig. 3B). Note the two major GPI-linked proteins of proteins ~35 and ~60 kDa (see arrows).

To biochemically detect only cell surface GPI-anchored proteins, we next used cell surface biotinylation and concentrated the biotinylated GPI-linked proteins by phase separation using the detergent Triton X-114 and precipitation with streptavidin agarose beads (see Materials and Methods). The recovered biotinylated GPI-linked proteins were then visualized via the proaerolysin overlay assay. We anticipated that only a subset of GPI-anchored proteins would be detected via this method, as they also must be lysine-rich proteins in order to be labeled by sulfo-NHS-biotin, which reacts only with free amino groups at the cell surface. Interestingly, using this approach in wild-type MEFs, we successfully detected the two major endogenous GPI-linked proteins (~35 and ~60 kDa; compare with Fig. 3B) at the cell surface (Fig. 3C, arrows). Importantly, visualization of these GPI-linked proteins was strictly dependent on cell surface biotinylation, as they were not observed if cell surface biotinylation was omitted (compare + and − lanes). In striking contrast, no cell surface GPI-linked proteins were detected in Cav-1 null MEFs (Fig. 3C), consistent with our findings from immunofluorescence microscopy (Fig. 2B). These data provide clear biochemical evidence that the two major endogenous GPI-linked proteins are not located at the cell surface in Cav-1 null MEFs.

To examine if this intracellular pool of GPI-linked proteins remains associated with lipid rafts, we also assessed their Triton solubility profile. Figure 3D shows that GPI-anchored proteins are predominantly Triton insoluble and that their distribution pattern is essentially identical both in wild-type and Cav-1 null MEFs.

Thus, we conclude that a loss of caveolin-1 expression does not affect the expression levels or raft-association of GPI-linked proteins. However, loss of caveolin-1 does result in the preferred intracellular retention of GPI-linked proteins in both lung tissue and cultured 3T3 fibroblasts.

Recombinant expression of caveolin-1 or caveolin-3 restores cell surface expression of GPI-linked proteins in Cav-1 null MEFs. Given that the absence of caveolin-1 expression causes the intracellular retention of GPI-linked proteins at the level of the Golgi, we speculated that we could rescue this trafficking defect by recombinantly expressing caveolin-1 in Cav-1 null MEFs. For this purpose, Cav-1 null MEFs were transiently transfected with the cDNA encoding caveolin-1.

Figure 4A shows that recombinant expression of caveolin-1 leads to the cell surface expression of GPI-linked proteins in Cav-1 null MEFs, successfully complementing the defect in their transport. Interestingly, caveolin-1 and GPI-linked proteins showed colocalization at the cell surface in caveolin-1-transfected cells. The same micrograph also shows two untransfected Cav-1 null MEFs in which GPI-anchored proteins are retained in the Golgi complex.

Currently, the caveolin gene family consists of caveolin-1, -2, and -3 (21). Caveolin-1 and -2 are coexpressed and form hetero-oligomeric complexes in many cell types (79, 81), while caveolin-3 is exclusively expressed in muscle cells (including skeletal, cardiac, and smooth muscle) (70, 89, 92). Therefore, we next examined whether transient expression of either caveolin-2 or caveolin-3 could rescue the cell surface expression of GPI-linked proteins.

FIG. 2. Intracellular retention of GPI-linked proteins in Cav-1-deficient 3T3 MEFs. (A) Caveolin Western blot analysis. 3T3 MEFs from Cav-1 knockout (KO) mice show an absence of caveolin-1 and severely reduced caveolin-2 levels. Samples containing 10 μg of lysates from wild-type (WT) and Cav-1 null MEFs were loaded in each lane, subjected to SDS-PAGE, and immunoblotted with an anti-Cav-1 MAb (clone 2297) or with an anti-Cav-2 MAb (clone 26). Equal protein loading was assessed using an anti-β-actin MAb. Results for two independent clones of each genotype are shown. (B) GPI cell surface labeling. Wild-type and Cav-1 null MEFs were grown on coverslips at a density of ~70 to 80% confluency. After fixation, the cells were not permeabilized. Instead, they were directly labeled with 10^{-8} M proaerolysin and then incubated with an anti-aerolysin MAb. Bound primary antibodies were visualized with an FITC-conjugated anti-mouse antibody (see Materials and Methods). Note that in wild-type MEFs, GPI-anchored proteins show a punctate pattern of cell surface staining, as expected. In striking contrast, Cav-1 null MEFs show little or no detectable cell surface labeling of GPI-linked proteins. (C and D) GPI staining after detergent permeabilization. Wild-type and Cav-1 null MEFs were grown on coverslips at a density of ~70 to 80% confluency. After fixation, the cells were permeabilized and then labeled with 10^{-8} M proaerolysin. Bound proaerolysin was visualized as described above in the legend for panel B. (C) In wild-type MEFs, GPI-anchored proteins were targeted to the plasma membrane and often assumed a polarized distribution. Arrows point at the cell surface. A longer exposure is also shown in the lower panel to illustrate the overall shape and contour of the cells. (D) In Cav-1 null MEFs, GPI-anchored proteins were primarily retained intracellularly in a perinuclear compartment (arrowheads). N, nucleus.

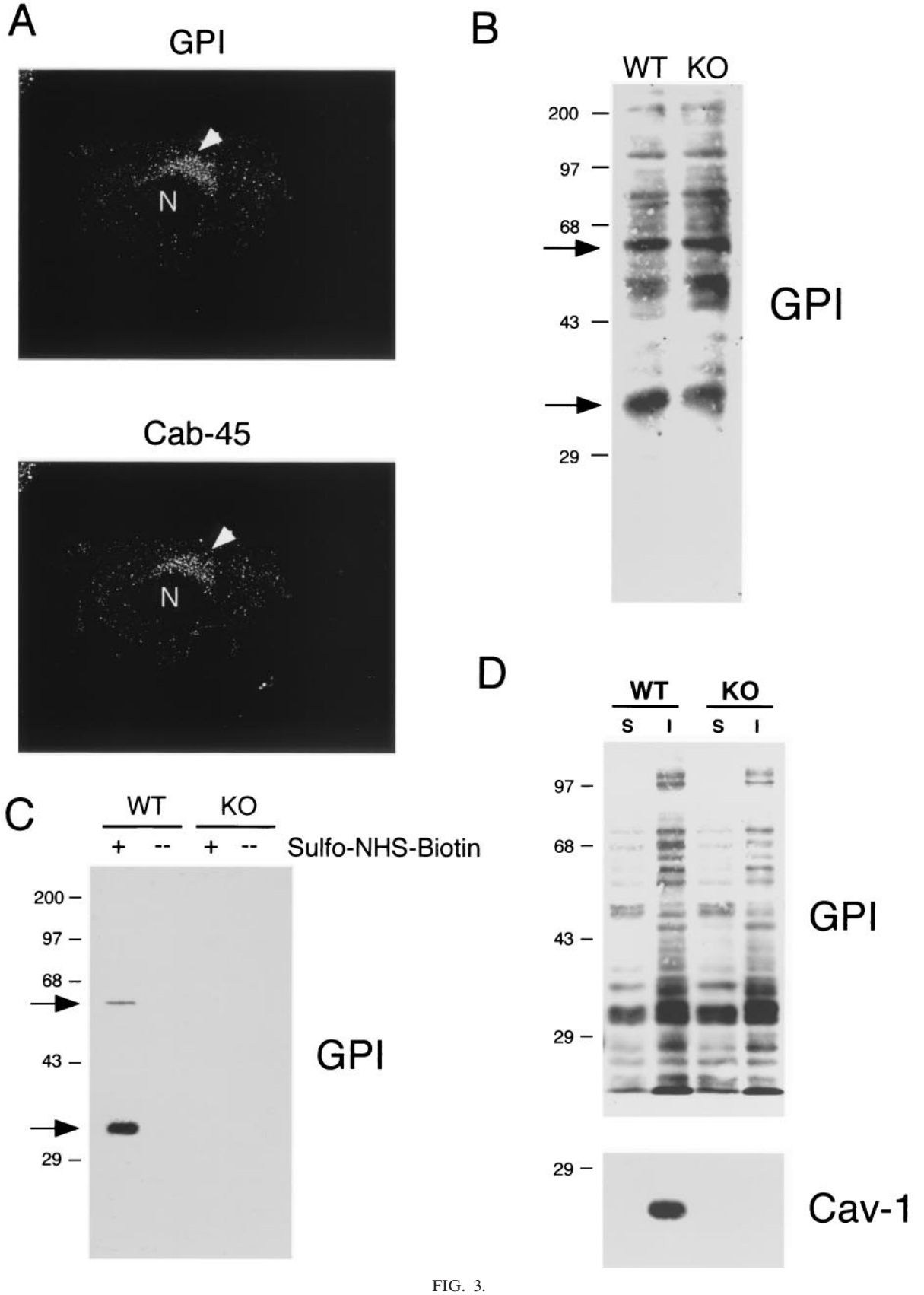
A
GPI
N
Cab-45
N
B
WT KO
200
97
68
43
29
GPI
C
WT KO
+ -- + --
Sulfo-NHS-Biotin
200
97
68
43
29
GPI
D
WT KO
S I S I
97
68
43
29
GPI
29
Cav-1

FIG. 3.

For this purpose, Cav-1 null MEFs were transiently transfected with the cDNAs encoding caveolin-2 or caveolin-3.

Figure 4B shows that recombinant expression of caveolin-2 could not compensate for caveolin-1's absence, as the GPI-linked proteins are still retained intracellularly. This is perhaps not surprising in light of recent evidence showing that in the absence of caveolin-1 expression, the stability and proper folding of the caveolin-2 protein is compromised. For example, in the absence of caveolin-1, caveolin-2 expression is greatly reduced via proteasomal degradation, residual caveolin-2 is trapped intracellularly at the level of the Golgi, and thus, caveolin-2 lacks the ability to induce caveola formation at the plasma membrane (59, 67, 72).

In contrast, Fig. 4C shows that recombinant expression of caveolin-3 rescued the ability of GPI-linked proteins to exit from the Golgi complex and to properly reach the cell surface. In this regard, it is interesting to note that caveolin-3, which has the highest homology to caveolin-1, is necessary and sufficient to induce the morphological formation of caveolae in muscle cells (28, 41). Thus, we conclude that expression of either caveolin-1 or caveolin-3 is required for the efficient transport of GPI-anchored proteins to the plasma membrane.

Expression of palmitoylated caveolin-1 is required for efficient transport of GPI-linked proteins to the plasma membrane in Cav-1 null MEFs. How does cytoplasmically oriented caveolin-1 interact with luminal GPI-linked proteins if they reside on opposite sides of the Golgi lipid bilayer? As caveolin-1 normally undergoes palmitoylation on three cysteine residues (133, 143, and 156) within its C-terminal domain (17), one possibility is that this interaction is mediated by the transbilayer association of the two or three fatty acyl groups on the GPI anchor with the three palmitoyl moieties attached to caveolin-1. The acyl group-dependent association of caveolin-1 with cholesterol (94) may also link the cytoplasmic and exoplasmic leaflets of the lipid bilayer, as cholesterol is present in both leaflets and can potentially form dimers that span the membrane, acting as a bridge (33) (Fig. 5A). Alternatively, palmitoylation of caveolin-1 may simply affect the global organization of lipid rafts, thereby facilitating the recruitment of GPI-linked proteins.

To test this hypothesis, we next examined the ability of a panel of four palmitoylation-deficient caveolin-1 mutants to rescue the cell surface expression of GPI-linked proteins in Cav-1 null MEFs. In these mutants, each caveolin-1 palmitoylation acceptor site is mutated from cysteine to serine (C133S, C143S, C156S, and the triple mutant C133, 143, 156S-Pal Minus) (Fig. 5B).

Importantly, palmitoylation-deficient caveolin-1 correctly forms high-molecular-mass oligomers and is correctly targeted to the plasma membrane/caveolae, behaving as wild-type caveolin-1 (17, 56, 94). However, this occurs despite the fact that palmitoylation-deficient caveolin-1 fails to recruit cholesterol to caveolar membranes (94). Similarly, it has been previously shown that all four of the caveolin-1 palmitoylation mutants used here correctly reach the plasma membrane and are correctly targeted to lipid rafts/caveolae (17, 94).

Figure 5C shows that palmitoylation-deficient caveolin-1 (C133, 143, 156S-Pal Minus) completely fails to rescue the cell surface transport of GPI-linked proteins. In order to further dissect this phenomenon, we next transiently transfected each caveolin-1 single mutant and analyzed the distribution of GPI-linked proteins by proaerolysin immunofluorescence. Interestingly, recombinant expression of caveolin-1 (C133S) was sufficient to recruit GPI-anchored proteins to the plasma membrane, although with a lower efficiency than wild-type caveolin-1 (Fig. 5D). In contrast, recombinant expression of caveolin-1 (C143S) or caveolin-1 (C156S) failed to rescue the cell surface expression of GPI-linked proteins (Fig. 5E and F). Thus, palmitoylation of caveolin-1 at cysteine residues 143 and 156 is most critical for caveolin-1 to functionally facilitate the cell surface transport of GPI-linked proteins. These results support the hypothesis that caveolin-1 palmitoyl groups somehow facilitate the clustering of GPI-linked proteins in Golgi-associated caveola-like vesicles that are then transported to the plasma membrane. Thus, palmitoylated caveolin-1 normally functions as a molecular escort to allow the efficient cell surface transport of GPI-linked proteins.

In Cav-3 null mice, GPI-anchored proteins are expressed at normal levels but display an abnormal localization pattern and are retained intracellularly. Our previous studies have demonstrated that Cav-3 null mice show various alterations in

FIG. 3. GPI-linked proteins are preferentially retained within lipid rafts at the level of the Golgi complex in Cav-1 null MEFs. (A) Double labeling with a Golgi marker protein. Formaldehyde-fixed and permeabilized Cav-1 null MEFs were double labeled with proaerolysin to visualize GPI-linked proteins and with Cab45, an endogenous Golgi marker protein. Bound primary antibodies were visualized with distinctly tagged secondary antibodies (see Materials and Methods). Note that the distributions of GPI-anchored proteins and Cab-45 precisely coincide, identifying the perinuclear region as the Golgi complex (arrowhead). N, nucleus. (B) GPI Western blot analysis. The expression levels of GPI-anchored proteins remained unchanged in Cav-1 null MEFs, compared with wild-type (WT) control MEFs. A 10-μg sample of cell lysate was loaded in each lane and separated by SDS-PAGE. The blots were subsequently subjected to proaerolysin overlay analysis to visualize GPI-linked proteins. Note the two major GPI-linked proteins with molecular masses of ~35 and ~60 kDa (see arrows). KO, knockout. (C) Biochemical detection of cell surface GPI-linked proteins. To detect only cell surface GPI-anchored proteins, we used cell surface biotinylation and concentrated the biotinylated GPI-linked proteins by phase separation using the detergent Triton X-114 and precipitation with streptavidin agarose beads (see Materials and Methods). The recovered biotinylated GPI-linked proteins were then visualized via the proaerolysin overlay assay. Note that by using this approach, we successfully detected the two major endogenous GPI-linked proteins (~35 and ~60 kDa; see arrows) at the cell surface in wild-type MEFs. Importantly, visualization of these GPI-linked proteins was strictly dependent on cell surface biotinylation, as they were not observed if cell surface biotinylation was omitted. In striking contrast, no cell surface GPI-linked proteins were detected in Cav-1 null MEFs. +, samples subjected to cell surface biotinylation with sulfo-NHS-biotin; −, the biotinylation step was omitted (a critical negative control). (D) GPI detergent insolubility. GPI-anchored proteins are detergent insoluble both in wild-type and knockout MEFs. After incubation of wild-type and Cav-1 null MEFs with a buffer containing 1% Triton X-100, the soluble fraction was collected. Then, the insoluble fraction was extracted using 1% SDS. Equal volumes of the soluble fraction and insoluble fraction were resolved by SDS-PAGE (10% acrylamide) and analyzed by proaerolysin overlay or caveolin-1 immunoblotting. Note that a caveolin-1 deficiency did not affect the detergent solubility of the GPI-anchored proteins; they remain predominantly Triton insoluble, indicative of their association with lipid rafts.

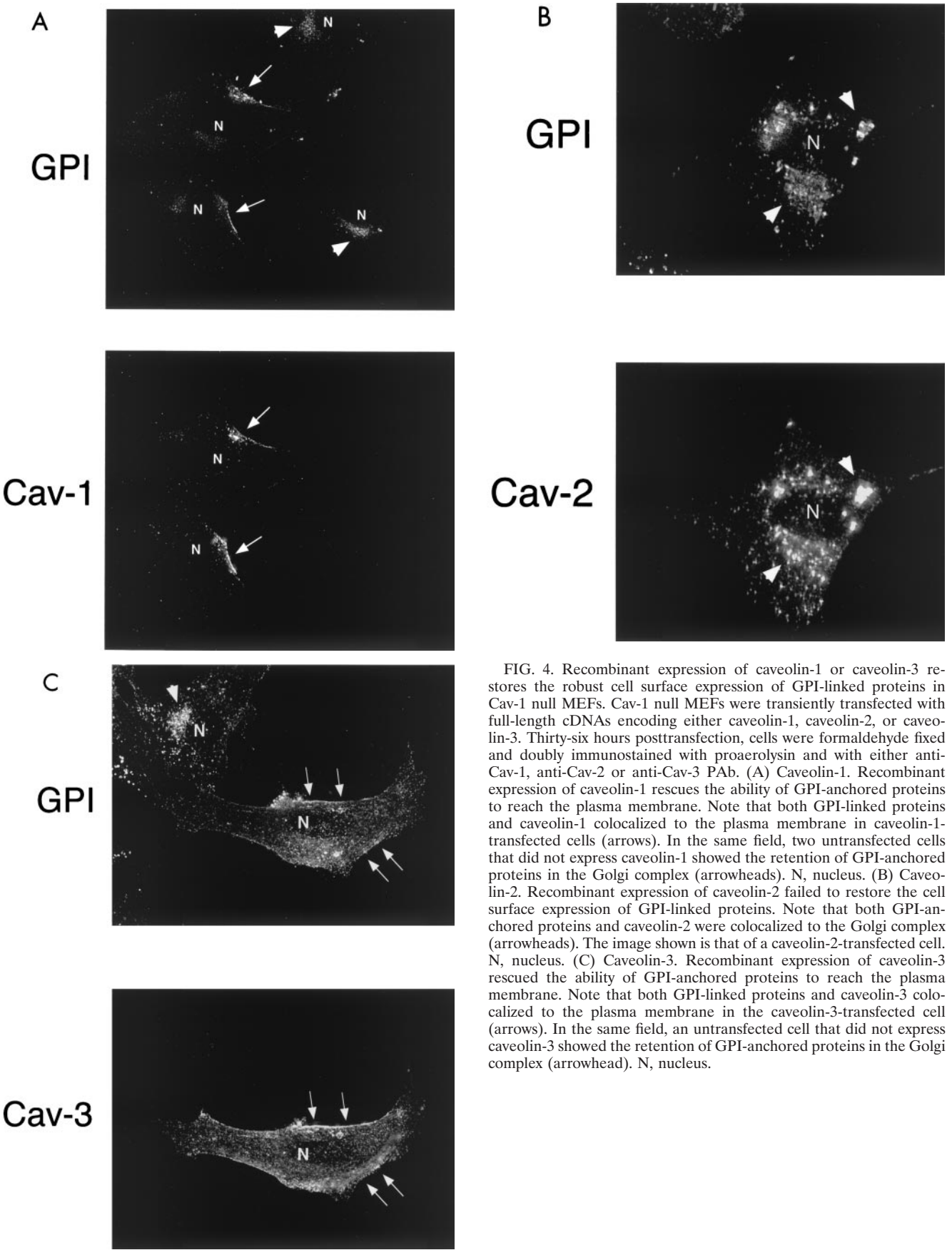

FIG. 4. Recombinant expression of caveolin-1 or caveolin-3 restores the robust cell surface expression of GPI-linked proteins in Cav-1 null MEFs. Cav-1 null MEFs were transiently transfected with full-length cDNAs encoding either caveolin-1, caveolin-2, or caveolin-3. Thirty-six hours posttransfection, cells were formaldehyde fixed and doubly immunostained with proaerolysin and with either anti-Cav-1, anti-Cav-2 or anti-Cav-3 PAb. (A) Caveolin-1. Recombinant expression of caveolin-1 rescues the ability of GPI-anchored proteins to reach the plasma membrane. Note that both GPI-linked proteins and caveolin-1 colocalized to the plasma membrane in caveolin-1-transfected cells (arrows). In the same field, two untransfected cells that did not express caveolin-1 showed the retention of GPI-anchored proteins in the Golgi complex (arrowheads). N, nucleus. (B) Caveolin-2. Recombinant expression of caveolin-2 failed to restore the cell surface expression of GPI-linked proteins. Note that both GPI-anchored proteins and caveolin-2 were colocalized to the Golgi complex (arrowheads). The image shown is that of a caveolin-2-transfected cell. N, nucleus. (C) Caveolin-3. Recombinant expression of caveolin-3 rescued the ability of GPI-anchored proteins to reach the plasma membrane. Note that both GPI-linked proteins and caveolin-3 colocalized to the plasma membrane in the caveolin-3-transfected cell (arrows). In the same field, an untransfected cell that did not express caveolin-3 showed the retention of GPI-anchored proteins in the Golgi complex (arrowhead). N, nucleus.

their skeletal muscle fibers, with a loss of sarcolemmal caveolae, a biochemical defect in the targeting of the dystrophin-dystroglycan complex to lipid rafts, and an immature disorganized T-tubule system (28). As we show here that recombinant expression of caveolin-3 in Cav-1 null MEFs is sufficient to rescue the cell surface expression of GPI-linked proteins, we wondered whether Cav-3 null mice also show defects in the trafficking of GPI-linked proteins in vivo.

Lysates from skeletal muscle tissue biopsies from wild-type and Cav-3 null mice were subjected to SDS-PAGE and proaerolysin overlays to detect GPI-linked proteins. Figure 6A shows that GPI-linked proteins are expressed at normal levels in skeletal muscle from Cav-3 null mice. Western blot analysis of the same samples was also performed using a caveolin-3-specific MAb probe to confirm that caveolin-3 expression is indeed absent in skeletal muscle from Cav-3 null mice.

Next, frozen sections were prepared from skeletal muscle biopsies taken from wild-type and Cav-3 null mice. These frozen sections were first stained with proaerolysin to visualize the distribution of GPI-linked proteins. A rabbit PAb directed against aerolysin was then used to detect bound proaerolysin in order to minimize secondary antibody cross-reactivity. Figure 6B shows that in skeletal muscle tissue sections from wild-type mice, GPI-linked proteins were localized to the sarcolemma (i.e., muscle cell plasma membrane), as expected. Interestingly, skeletal muscle fibers from Cav-3 null mice displayed significant changes in the distribution of GPI-anchored proteins. Note the intracellular retention of GPI-linked proteins in Cav-3 null skeletal muscle fibers; in contrast, the neighboring endothelial cells which express caveolin-1 showed a normal labeling pattern.

We next immunostained these skeletal muscle frozen sections with antibodies to T-cadherin, an endogenously expressed GPI-linked protein that plays a role in cell-cell adhesion in muscle. In contrast to the classical cadherins, T-cadherin does not possess transmembrane and cytosolic domains and is instead attached to the cell membrane by a GPI anchor (2). Recent studies have shown that T-cadherin localizes within caveolin-rich membrane domains in vascular smooth muscle cells (71). Interestingly, staining either with proaerolysin or with a specific PAb directed against T-cadherin showed a similar immunostaining pattern (Fig. 6C). Note that in Cav-3 null mice, the skeletal muscle fibers show significant intracellular retention of T-cadherin. As expected, T-cadherin was localized to the muscle cell plasma membrane in wild-type muscle fibers.

As an important internal control, we also assessed the immunoreactivity of our samples by using antibodies to β-dystroglycan. We chose β-dystroglycan since it is a ubiquitous membrane protein that we have previously shown to be expressed at normal levels at the sarcolemma in Cav-3 null mice (28). Note that, as expected, the overall sarcolemmal localization of β-dystroglycan is not affected in caveolin-3 null mice (Fig. 6D).

We conclude that in Cav-3 null mice, GPI-anchored proteins are expressed at normal levels but display an abnormal localization pattern and are retained intracellularly. These results directly support our observations obtained with Cav-1 null MEFs.

Intracellular retention of GPI-linked protein in the renal tubules of Cav-1 null mice. As GPI-linked proteins are selectively targeted to the apical surface of polarized renal epithelial cells in culture (7, 44, 49, 51), we next examined the expression and the distribution of GPI-anchored proteins in the renal tubules of the kidney in vivo. First, the kidneys were harvested, and lysates were prepared to examine the expression levels of GPI-linked proteins by SDS-PAGE and proaerolysin overlays. Interestingly, no changes in the expression of GPI-linked proteins were observed in kidneys derived from Cav-1 null mice (Fig. 7A). Western blot analysis of the same samples was also performed using a caveolin-1-specific PAb probe to confirm that caveolin-1 expression was indeed absent in kidney from Cav-1 null mice.

Kidney paraffin sections from wild-type and Cav-1 null mice were generated and immunostained with antibodies directed against a specific renal tubule GPI-anchored protein, Tamm-Horsfall, which is also known as the major urinary glycoprotein (13, 74). Figure 7B shows that the Tamm-Horsfall protein was properly localized at the apical surface of renal tubular epithelial cells and shows a ring-like staining pattern in the wild-type mice, as expected. In contrast, the Tamm-Horsfall protein is largely excluded from this location and is mainly found intracellularly in Cav-1 null mice.

Thus, it appears that caveolin-deficient mice show a pleiotropic defect in the cell surface transport of GPI-linked proteins.

Perinuclear retention of c-Src in Cav-1-deficient MEFs: recombinant expression of caveolin-1 restores the normal plasma membrane distribution of c-Src. As GPI-linked proteins are retained in lipid rafts at the level of the Golgi complex in Cav-1 null MEFs, we wondered whether other lipid raft marker proteins might suffer a similar fate. Thus, we next examined the distribution of c-Src, a member of the Src family of tyrosine kinases and a cytoplasmic lipid raft marker protein (88) in Cav-1 null MEFs. If c-Src is retained in an intracellular compartment as well, this might suggest that lipid rafts themselves may be preferentially retained intracellularly in Cav-1 null MEFs.

To facilitate the detection of c-Src, wild-type and Cav-1 null MEFs were transiently transfected with the cDNA encoding the human c-Src protein and were subjected to analysis by immunofluorescence microscopy using anti-Src IgG. Figure 8A shows that in wild-type MEFs, c-Src resided at the plasma membrane, as expected. In contrast, in Cav-1 null MEFs, c-Src was preferentially retained at an intracellular perinuclear site that we identified as the Golgi complex (Fig. 8A; data not shown).

Importantly, the intracellular retention of c-Src could be rescued by the recombinant expression of caveolin-1 in Cav-1 null MEFs (Fig. 8B). However, palmitoylation-deficient caveolin-1 (C133, 143, 156S-Pal Minus) showed little or no ability to rescue the plasma membrane targeting of c-Src (Fig. 8C and D). Thus, we conclude that palmitoylation of caveolin-1 is normally required for the efficient cell surface transport of lipid rafts that contain GPI-linked proteins and Src family kinases. In this regard, Golgi-associated caveolins and caveola-like vesicles could represent part of the transport machinery that is necessary for efficiently moving lipid rafts and their associated proteins from one cellular compartment to the next—in this case, from the Golgi to the plasma membrane.

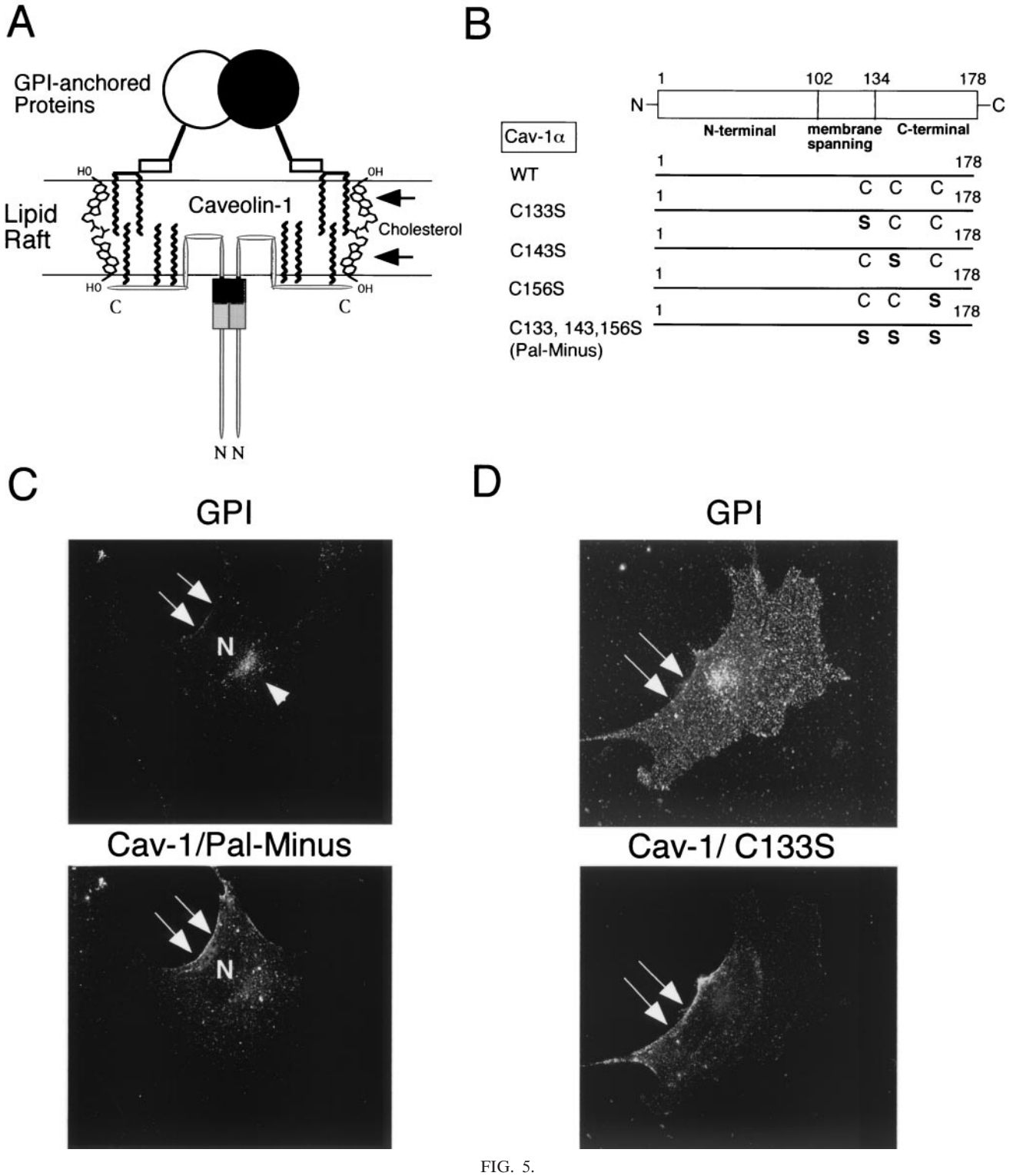

FIG. 5.

Consistent with these findings, we have previously shown that palmitoylation of caveolin-1 is required for caveolin-1 to be tyrosine phosphorylated by c-Src in transiently transfected Cos-7 cells (38); however, we did not evaluate the subcellular distribution of c-Src in these transfected Cos-7 cells. Thus, our current findings using caveolin-1-deficient fibroblasts provide a novel molecular explanation for this uncoupling event, as we now show that c-Src is retained in the Golgi, while palmitoylation-deficient caveolin-1 localizes to the plasma membrane.

Clustering and internalization of CT-B is impaired in Cav-1

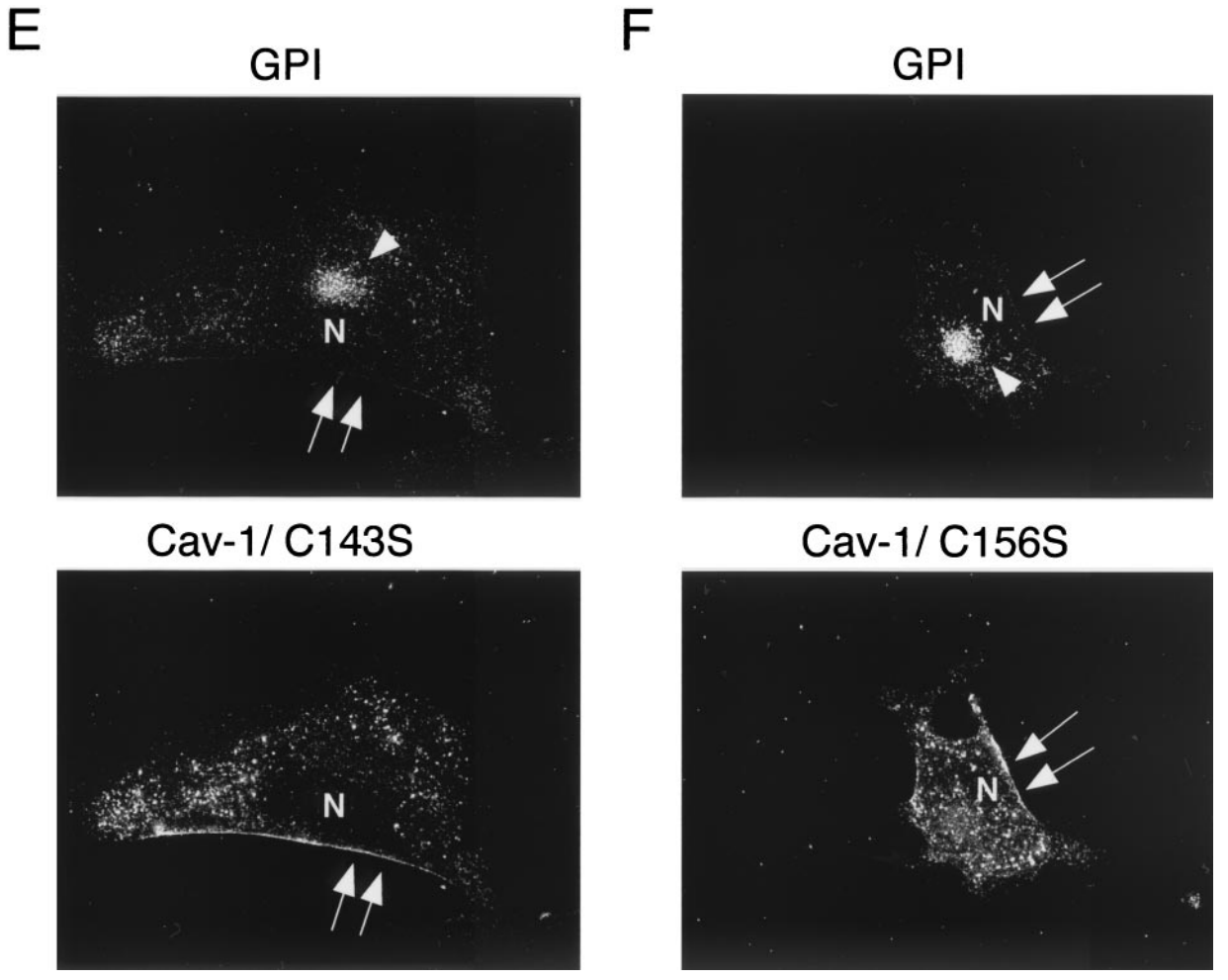

FIG. 5. Expression of palmitoylated caveolin-1 is required for efficient transport of GPI-linked proteins to the plasma membrane in Cav-1 null MEFs. (A) Schematic diagram. GPI-linked proteins are confined to the exoplasmic leaflet of the membrane, while caveolins are cytoplasmically oriented membrane proteins. As caveolin-1 normally undergoes palmitoylation on three cysteine residues (133, 143, and 156), we speculate that caveolin-1 palmitoylation might mechanistically serve to couple caveolin-1 to GPI-linked proteins. In direct support of this hypothesis, in vivo chemical cross-linking studies with an iodinated derivative of GM_1 (a glycosphingolipid) showed that GM_1 interacted directly with caveolin-1 in intact cells, despite the fact that GM_1 (exoplasmic) and caveolin-1 (cytoplasmic) are on opposite sides of the lipid bilayer (25). The acyl group-dependent association of caveolin-1 with cholesterol (94) may also link the cytoplasmic and exoplasmic leaflets of the lipid bilayer, as cholesterol is present in both leaflets and can potentially form dimers that span the membrane-acting as a bridge (33). Alternatively, palmitoylation of caveolin-1 may simply affect the global organization of lipid rafts, thereby indirectly facilitating the recruitment of GPI-linked proteins. (B) Palmitoylation-deficient caveolin-1 mutants. A representation of the N-terminal, membrane-spanning, and C-terminal domains of caveolin-1 is shown. Each cysteine residue within caveolin-1 that is normally palmitoylated was mutated to a serine, either individually or in combination. (C to F) GPI staining after detergent permeabilization. Cav-1 null MEFs were transfected with each of the full-length cDNAs encoding the above indicated caveolin-1 palmitoylation mutants. Thirty-six hours posttransfection, cells were formaldehyde fixed and doubly immunostained with proaerolysin and with an anti-caveolin-1 PAb (N20). Note that palmitoylation-deficient caveolin-1 (C133, 143, and 156S-Pal Minus) completely failed to rescue the cell surface transport of GPI-linked proteins. However, recombinant expression of caveolin-1 (C133S) was sufficient to recruit GPI-anchored proteins to the plasma membrane, although with a lower efficiency than wild-type caveolin-1. In contrast, recombinant expression of caveolin-1 (C143S) and caveolin-1 (C156S) failed to rescue the cell surface expression of GPI-linked proteins. Thus, palmitoylated caveolin-1 normally functions as a molecular escort to allow the efficient cell surface transport of GPI-linked proteins. (C to F) Arrows point at the cell surface, while arrowheads point at the Golgi complex. N, nucleus.

null MEFs. Since the other lipid raft markers that we tested were retained intracellularly in Cav-1 null MEFs (GPI-linked proteins and c-Src), we searched for a lipid raft marker that still remained at the cell surface. This would then allow us to assess the effect of a loss of caveolin-1 on the clustering and internalization of lipid rafts at the cell surface. Interestingly, the binding of CT-B to the cell surface of Cav-1 null cells was essentially the same as in wild-type MEFs. CT-B specifically binds GM_1, an abundant cell surface glycosphingolipid, and is normally internalized via plasmalemmal caveolae, as visualized by electron microscopy (58, 69). As such, CT-B has been extensively used by fluorescence microscopy as a cell surface lipid raft marker to follow the internalization of GM_1 (34, 64). In addition, in vivo chemical cross-linking studies with an iodinated derivative of GM_1 showed that GM_1 interacts directly with caveolin-1 in intact cells, despite the fact that GM_1 (exoplasmic) and caveolin-1 (cytoplasmic) are on opposite sides of the lipid bilayer (25). Furthermore, the efficiency of the chem-

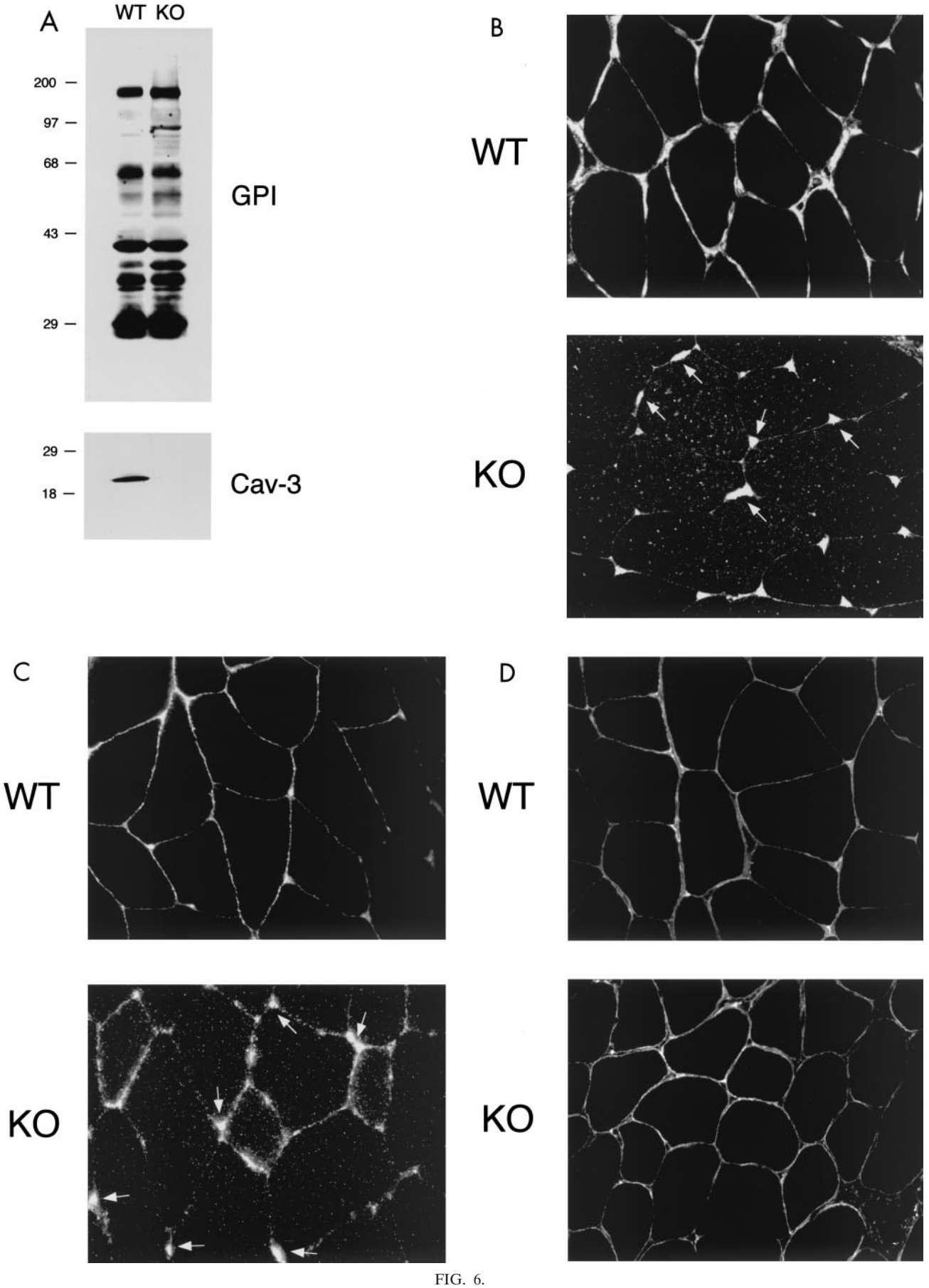

FIG. 6.

ical cross-linking of photoreactive GM_1 to caveolin-1 is increased by ~5-fold by the addition of CT-B, a pentameric molecule (25).

Figure 9 shows the behavior of cell surface-bound CT-B in wild-type and Cav-1 null MEFs. In wild-type cells, the clustering and internalization of CT-B was apparent after 15 to 30 min and was nearly complete by 45 min. After 45 min, CT-B accumulated intracellularly in a perinuclear compartment (Fig. 9A and B, left), as expected. In contrast, Cav-1 null MEFs clearly showed impaired clustering and internalization of CT-B. Little or no clustering of CT-B occurred at 15 to 30 min, and by 45 min, there was little or no accumulation in a perinuclear compartment. The efficient internalization of CT-B in Cav-1 null cells was rescued by recombinant expression of the caveolin-1 cDNA (data not shown). Thus, caveolin-1 is also required for the efficient internalization of lipid raft markers at the cell surface.

The present findings for cholera toxin, a membrane-bound ligand, are consistent with our previously published studies showing that the internalization of the protein albumin, a soluble ligand, is blocked in (i) primary cultures of Cav-1 null MEFs in vitro (72) and (ii) Cav-1 null endothelial cells in vivo (84). In addition, they support the hypothesis that caveolin-1-containing vesicles function both in the endocytic and exocytic transport of certain lipid raft-associated molecules. Furthermore, these studies make it highly unlikely that the intracellular retention of GPI-linked proteins that we observed for Cav-1 null 3T3 MEFs is due to their rapid endocytosis from the cell surface.

In addition, other groups have suggested that the internalization of cholera toxin is independent of caveolin-1 and caveolae, but they have used overexpression systems or highly transformed cell lines (3, 65, 85, 93). Thus, our experiments presented here were conducted under more physiologically relevant circumstances and clearly demonstrate that the internalization of cholera toxin is a caveolin-dependent process.

DISCUSSION

The mechanisms underlying the sorting and vesicular transport of GPI-anchored proteins are largely unknown. It has been observed that GPI-linked proteins partition into lipid rafts at the level of the trans-Golgi, as revealed by their resistance to solubilization by nonionic detergents at low temperatures. However, it remains unknown how these lipid raft-associated GPI-linked proteins are clustered, packaged, and transported to the plasma membrane. One attractive hypothesis is that lipid rafts containing GPI-linked proteins are incorporated into Golgi-associated caveola-like vesicles for transport to the plasma membrane. This hypothesis was first proposed in the early 1990s (45, 54, 78); however, it remained untested until now.

Here, we exploited a new experimental model system that allowed us to test this hypothesis directly. Recently, we and others generated Cav-1 null mice (72). Fibroblasts derived from their embryos (MEFs) represent the ideal tool to study the role of caveolins in GPI-linked protein sorting. These Cav-1 null MEFs lack morphological caveolae, do not express caveolin-1, and show a ~95% down-regulation in caveolin-2 expression (72); these cells also do not express caveolin-3, a muscle-specific caveolin family member (72). As such, these cells are truly deficient in caveolins and caveolae.

Using these Cav-1 null MEFs, we show that GPI-linked proteins are expressed at normal levels and are still associated with lipid rafts, as judged by their resistance to solubilization by Triton X-100 at low temperature. However, these GPI-linked proteins are retained intracellularly in a perinuclear compartment that we identify as the Golgi complex. Interestingly, the recombinant expression of caveolin-1 in Cav-1 null MEFs can correct this phenotype and rescue the ability of GPI-linked proteins to reach the cell surface. Thus, expression of caveolin-1 is normally required for the efficient transport of GPI-linked proteins to the cell surface. These results directly support the hypothesis that lipid rafts containing GPI-linked proteins are normally incorporated into Golgi-derived caveola-like vesicles and transported to the plasma membrane. Our present results are also entirely consistent with the original identification of caveolin-1 as a component of trans-Golgi derived transport vesicles (19, 37). They also suggest that caveolin-1 may move among various membranous compartments because it has affinities for several distinct lipid microenvironments.

As caveolin-1 is only the first member of a gene family, we tested whether recombinant expression of the other two members of this family, namely caveolin-2 and -3, can exert a similar effect. And indeed, caveolin-3 expression, but not that of caveolin-2, can restore the cell surface expression of GPI-anchored proteins in Cav-1 null MEFs. Further evidence is provided by our analysis of Cav-3 null mice, as skeletal muscle fibers derived from these mice displayed an altered pattern of GPI-linked protein localization, with the accumulation of a significant intracellular pool of GPI-linked proteins. Based on these findings, we can conclude that caveolin-1 and caveolin-3, but not caveolin-2, are both independently required for the efficient cell surface transport of GPI-anchored proteins, depending on the tissues where they are expressed. Several independent lines of evidence also now indicate that expression

FIG. 6. In Cav-3 null mouse skeletal muscle fibers, GPI-anchored proteins are expressed at normal levels but display an abnormal localization pattern and are retained intracellularly. (A) GPI Western blot analysis. Protein lysates were prepared from skeletal muscle biopsies taken from wild-type (WT) and Cav-3 null (KO) mice. After SDS-PAGE and transfer to nitrocellulose, the blots were subjected to proaerolysin overlay to detect GPI-linked proteins or to caveolin-3 immunoblotting. Note that the GPI-anchored proteins were expressed at normal levels in the skeletal muscle of Cav-3 null mice, compared to those of wild-type control mice. (B to D) Immunohistochemistry. Skeletal muscle tissue frozen sections were prepared from wild-type and Cav-3 null mice. These frozen sections were then immunostained with (i) proaerolysin to reveal the distribution of GPI-linked proteins (B), (ii) a PAb directed against T-cadherin, an endogenous GPI-linked protein that is prominently expressed in skeletal muscle (C), or (iii) a MAb directed against β-dystroglycan (D). Note the intracellular retention of GPI-linked proteins (B and C) in Cav-3 null skeletal muscle fibers; in contrast, the neighboring endothelial cells (arrows) which express caveolin-1 showed a normal labeling pattern.

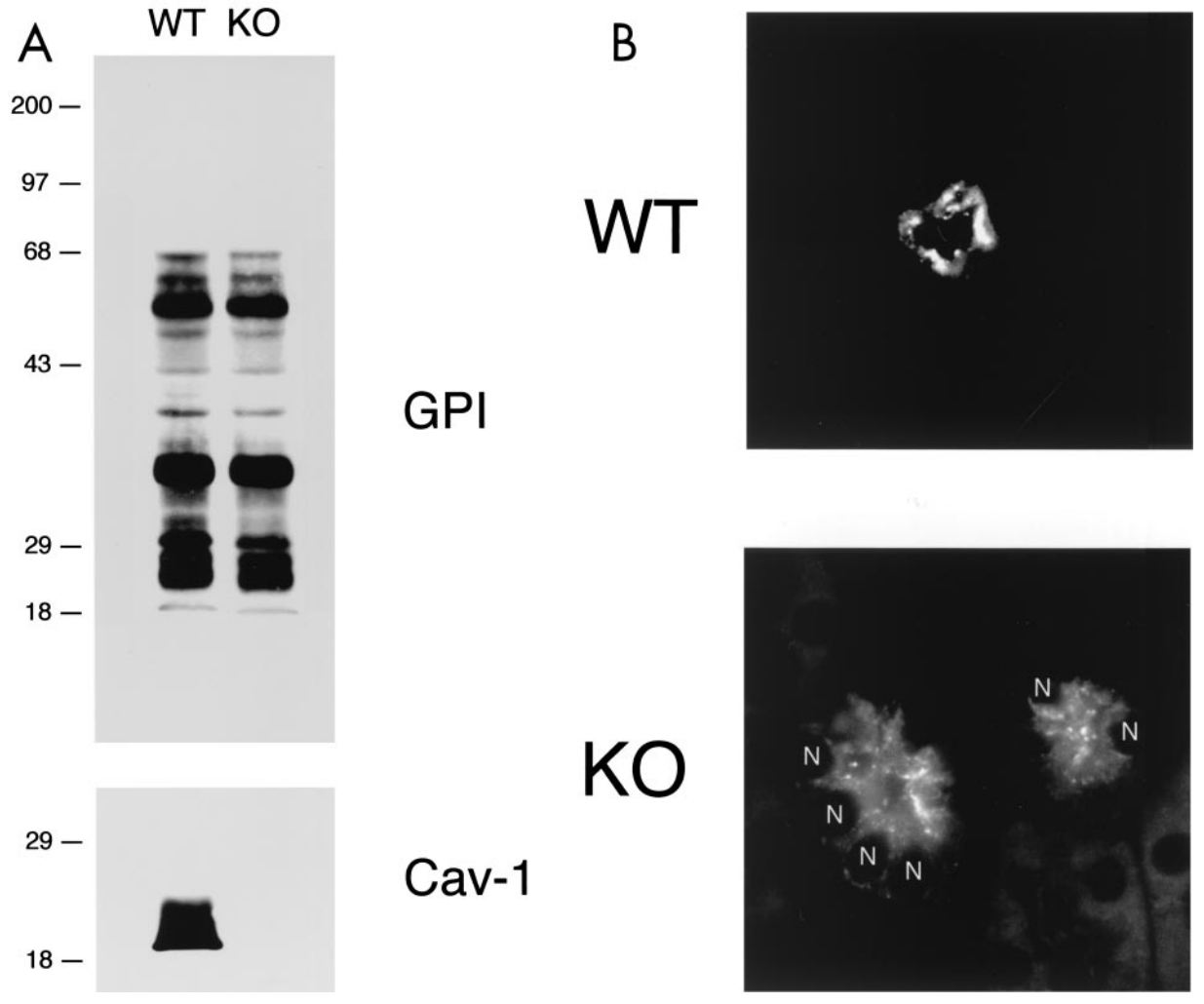

FIG. 7. Intracellular retention of GPI-linked proteins in the renal tubules of Cav-1 null mice. (A) GPI Western blot analysis. Protein lysates were prepared from kidneys harvested from wild-type (WT) and Cav-1 null (KO) mice. After SDS-PAGE and transfer to nitrocellulose, the blots were subjected to proaerolysin overlay to detect GPI-linked proteins or to caveolin-1 immunoblotting. Note that the GPI-anchored proteins were expressed at normal levels in the kidneys of Cav-1 null mice, compared to those of wild-type control mice. (B) Tamm-Horsfall immunostaining. Kidney paraffin sections prepared from wild-type and Cav-1 null mice were immunostained with a polyclonal sheep antibody directed against the Tamm-Horsfall protein, a GPI-anchored protein endogenously expressed in the renal tubules. Note that in wild-type mice, the Tamm-Horsfall protein was properly localized at the apical cell surface of renal tubular epithelial cells and showed a ring-like staining pattern, as expected. In contrast, in Cav-1 null mice, the Tamm-Horsfall protein was largely excluded from the apical plasma membrane and was found mainly intracellularly in a vesicular perinuclear compartment that was proximal to the apical cell surface. N, nucleus.

FIG. 8. Perinuclear retention of c-Src in Cav-1-deficient MEFs: recombinant expression of caveolin-1 restores the normal plasma membrane distribution of c-Src. (A) c-Src immunostaining. Wild-type (WT) and Cav-1 null (KO) MEFs were transiently transfected with the cDNA encoding c-Src. Cells were then fixed, permeabilized, and immunolabeled with a specific antibody directed against c-Src. Note that in wild-type MEFs, c-Src resided at the plasma membrane, as expected. In contrast, in Cav-1 null MEFs, c-Src was preferentially retained at an intracellular perinuclear site. (B) Wild-type caveolin-1. Cav-1 null MEFs were cotransfected with the cDNAs encoding c-Src and wild-type caveolin-1. c-Src expression was detected with a specific mouse MAb; caveolin-1 expression was detected with a rabbit PAb (N-20). Bound primary antibodies were visualized by incubation with distinctly tagged fluorescent secondary antibodies. Cells expressing both transfected gene products were selected for imaging. Note that expression of wild-type caveolin-1 restored the normal plasma membrane distribution of c-Src. (C and D) Palmitoylation-deficient caveolin-1. Cav-1 null MEFs were cotransfected with the cDNAs encoding c-Src and palmitoylation-deficient (C133, 143, and 156S-Pal Minus) caveolin-1. The recombinant expression of c-Src and caveolin-1 was detected as described above for panel B. Note that palmitoylation-deficient caveolin-1 showed little (C) or no (D) ability to rescue the plasma membrane targeting of c-Src. Thus, we conclude that palmitoylation of caveolin-1 is normally required for the efficient cell surface transport of lipid rafts that contain GPI-linked proteins and Src-family kinases. (A to C) Arrows point at the cell surface, while arrowheads point at the Golgi complex. N, nucleus.

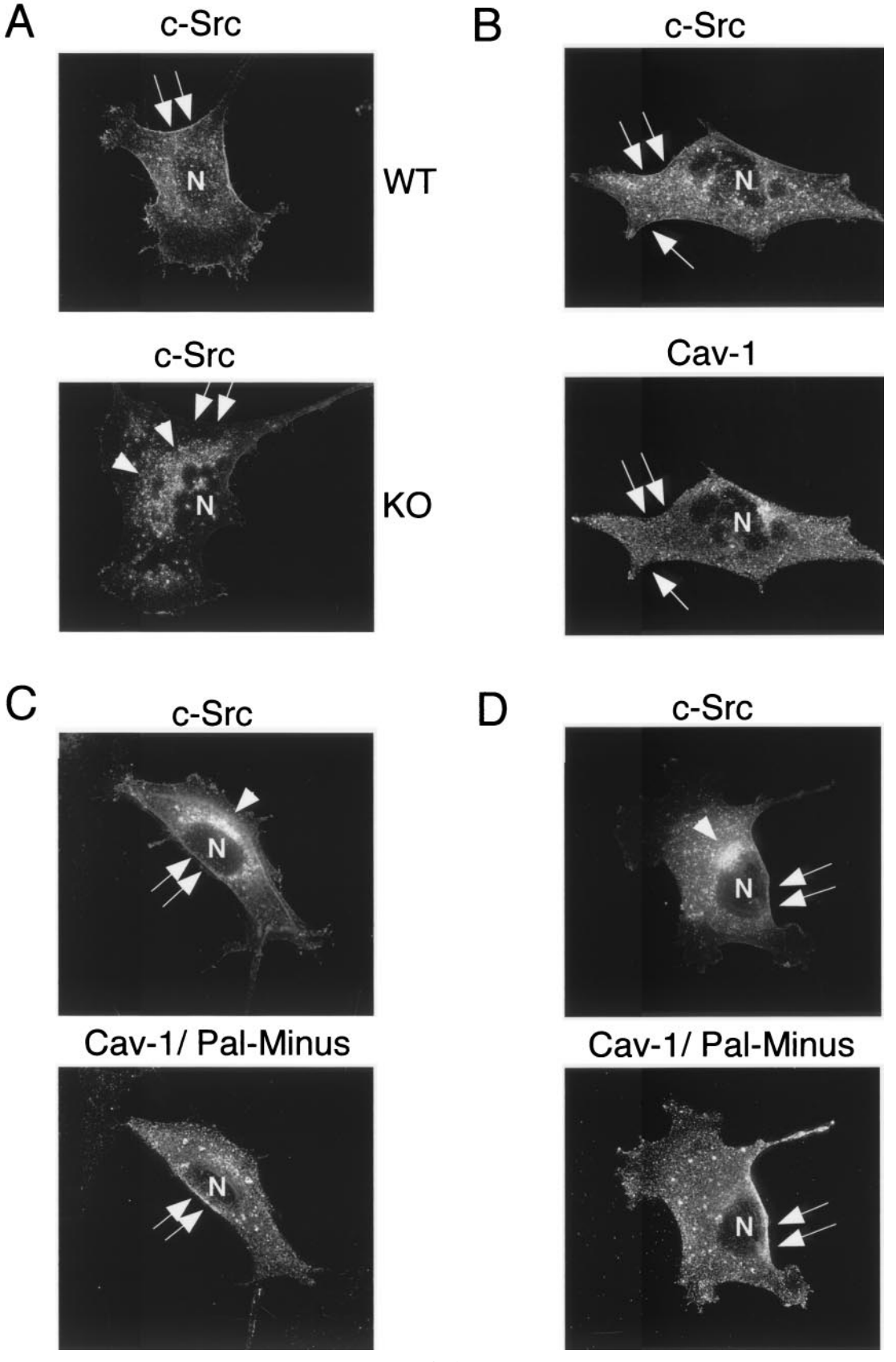
A
c-Src
N
WT
c-Src
N
KO
B
c-Src
N
Cav-1
N
C
c-Src
N
Cav-1/ Pal-Minus
N
D
c-Src
N
Cav-1/ Pal-Minus
N

FIG. 8.

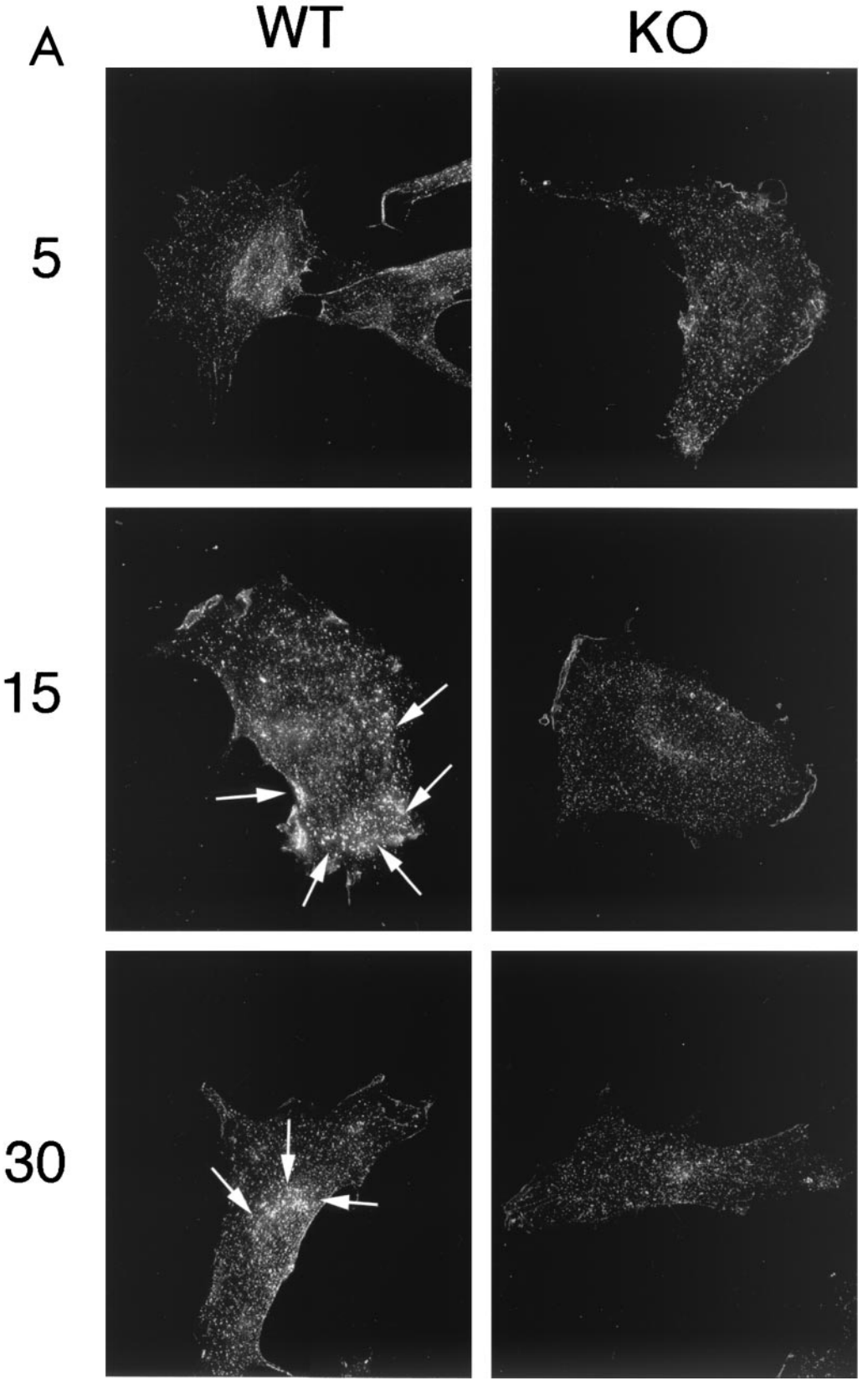

FIG. 9. Clustering and internalization of CT-B is impaired in Cav-1 null MEFs. Wild-type and Cav-1 null 3T3 MEFs were incubated with CT-B for 30 min on ice, unbound material was removed, and the cells were then warmed to 37°C to allow clustering and internalization to occur. CT-B binding and internalization were visualized by immunostaining with anti-CT IgG. (A) MEFs after 5, 15, and 30 min of internalization. Note that the cell surface clustering and internalization of CT-B was clearly impaired in Cav-1 null (KO) MEFs. Arrows point at areas of cell surface clustering and internalization in wild-type (WT) MEFs. (B) MEFs after 45 min of internalization. Note that little or no cell surface clustering and internalization was apparent in Cav-1 null MEFs. In contrast, by 45 min, internalization of CT-B in wild-type MEFs was virtually complete, with a high concentration of CT-B accumulating in a perinuclear compartment (arrows).

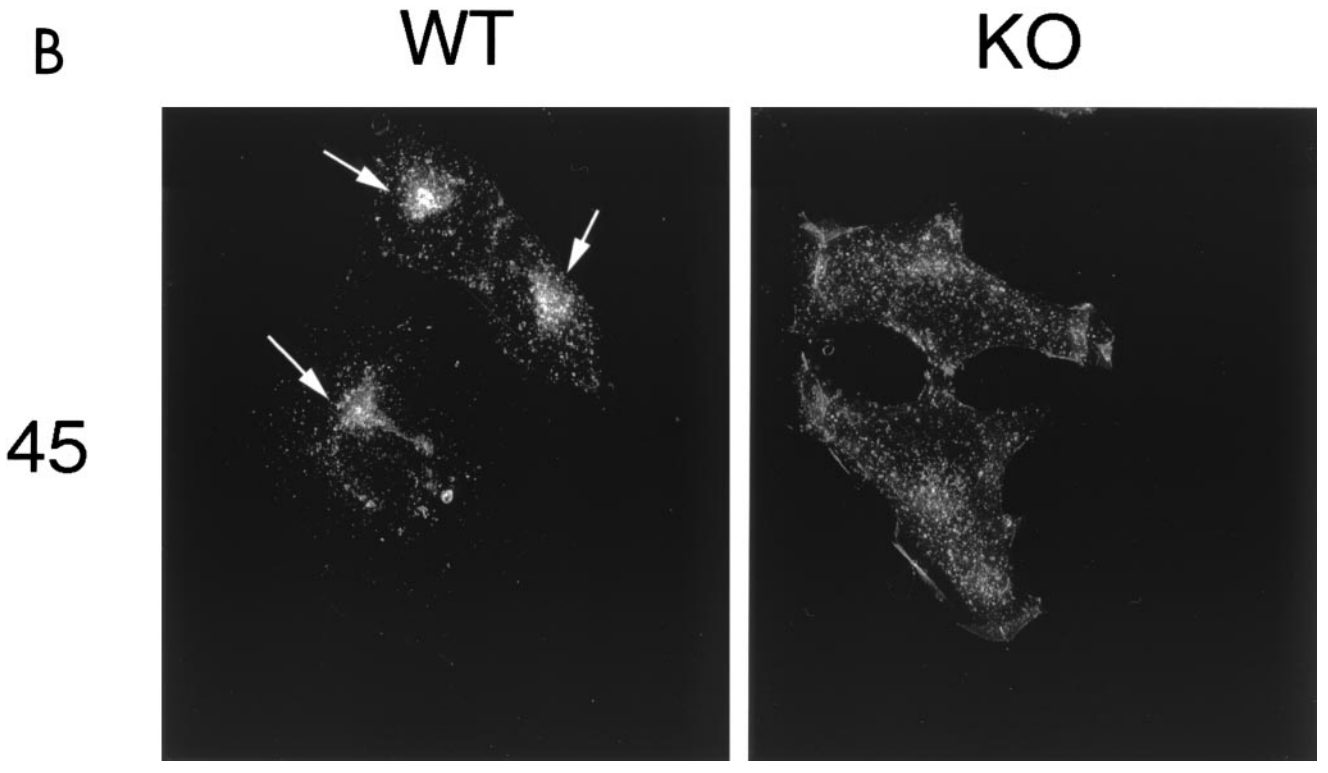

FIG. 9—*Continued*.

of either caveolin-1 or caveolin-3, but not of caveolin-2, is sufficient to drive formation of caveolae (18, 20, 26, 28, 32, 41, 42, 59, 72). These results strongly suggest a functional interdependence between caveolin expression, formation of caveolae, and GPI-anchored protein transport to the cell surface.

In order to dissect the mechanisms underlying the intracellular retention of GPI-linked proteins in Cav-1 null MEFs, we explored the hypothesis that lipid-lipid interactions between caveolin-1 and GPI-anchored proteins could play a prominent role in the biosynthetic targeting of GPI-linked proteins to the cell surface. Lipid modification of certain proteins, for example, c-Src but surprisingly not caveolin-1 itself, is an essential feature for caveolar targeting (10, 17, 88). Nevertheless, palmitoylation of caveolin-1 is required for its coupling to the c-Src tyrosine kinase (39) and for cholesterol binding (94). In the present study, we show that palmitoylation of caveolin-1 at Cys-143 and Cys-156 is required for caveolin-1 to complement the defect in the cell surface transport of GPI-linked proteins in Cav-1 null MEFs. Thus, we speculate that the lipid moiety of the GPI anchor and the caveolin-1 palmitoyl groups somehow interact with each other across the bilayer to allow the clustering of GPI-linked proteins in Golgi-associated caveola-like vesicles that are then transported to the plasma membrane. The acyl group-dependent association of caveolin-1 with cholesterol (94) may also link the cytoplasmic and exoplasmic leaflets of the lipid bilayer, as cholesterol is present in both leaflets and can potentially form dimers that span the membrane (33), thus acting as a bridge (Fig. 5A). Alternatively, palmitoylation of caveolin-1 may simply affect the global organization of lipid rafts, thereby indirectly facilitating the recruitment of GPI-linked proteins.

We then speculated that perhaps Golgi-associated caveola-like vesicles could act as vesicular carriers for "shipping" other lipid raft-associated "cargo" molecules to the cell surface. To test this hypothesis, we next examined the trafficking of c-Src in Cav-1 null MEFs. c-Src and other Src family tyrosine kinases undergo lipid modifications, such as myristoylation and palmitoylation, that act as targeting signals for partitioning cytoplasmic signaling molecules into lipid rafts and caveolae. Using Cav-1 null MEFs, we show that, like GPI-anchored proteins, c-Src is preferentially retained at an intracellular perinuclear site that we identified as the Golgi complex. Interestingly, intracellular retention of c-Src was rescued by recombinant expression of caveolin-1. However, palmitoylation-deficient caveolin-1 showed little or no ability to rescue the plasma membrane targeting of c-Src. Thus, Golgi-associated caveolins and caveola-like vesicles may represent part of the transport machinery that is necessary for efficiently moving lipid rafts and their associated proteins from the Golgi to the plasma membrane.

These findings are consistent with our recent observation that palmitoylation of caveolin-1 is required for its coupling to the c-Src tyrosine kinase at the cell surface, as assessed using the tyrosine phosphorylation of caveolin-1 (pY14) as an in vivo measure of this association (39). Importantly, the Src-mediated tyrosine phosphorylation of caveolin-1 could be competitively uncoupled by the antibody-induced clustering of GPI-linked proteins within caveolae at the cell surface (39). As GPI-acyl

groups are restricted to the exoplasmic leaflet of the lipid bilayer, while caveolin-1 palmitoyl groups and the c-Src myristoyl group reside within the cytoplasmic leaflet of the lipid bilayer, these results provide further evidence that there is communication between lipid moieties within the exoplasmic and cytoplasmic leaflets of the lipid bilayer. Thus, similar interactions operating at the cell surface or within the Golgi complex could possibly mediate the association of GPI-linked proteins with caveola-like vesicles and the caveolin proteins.

Our present results may also explain the effects of activated Ras proteins on the trafficking of endogenous GPI-linked proteins in fibroblastic cells. At least two previous reports have documented the loss of cell surface expression of GPI-linked proteins in H-Ras-transformed NIH 3T3 cells (4, 35). In addition, we have previously shown that caveolin-1 protein expression and caveolae are dramatically down-regulated or absent in H-Ras (G12V)-transformed NIH 3T3 cells (20, 36); constitutive activation of the Ras-p42/44-MAP kinase pathway leads to substantial decreases in caveolin-1 mRNA levels and directly inhibits caveolin-1 gene transcription, as shown using caveolin-1 promoter–luciferase reporter constructs (22). Thus, loss of cell surface expression of GPI-linked proteins in Ras-transformed NIH 3T3 cells may be due to the down-regulation of caveolin-1 protein expression and caveolae in these cells.

Finally, although the expression of caveolins 1 and 2 is relatively ubiquitous, clearly not all cells express the caveolin proteins. For example, it has been shown that T lymphocytes possess cell surface pools of GPI-linked proteins that participate in signal transduction, but T cells fail to express any known caveolin family members and lack caveolae (26, 27, 68). Thus, other functional homologues of the caveolins must exist to direct the cell surface transport of GPI-linked proteins and other lipid raft components in cells that normally do not express caveolin gene family members. The search for such functional homologues of the caveolins will be greatly facilitated by the use of the 3T3–Cav-1–null MEF complementation system that we describe herein. By analogy with the caveolins, we predict that such functional homologues will be oligomeric lipid-modified integral membrane proteins that partition into lipid rafts.

Recently, Nichols et al. (63) demonstrated that rapid cycling of a transiently transfected minimal GPI-linked protein (GPI-green fluorescent protein) between the Golgi apparatus and the cell surface may occur. However, the caveolin-1-dependence of this phenomenon was not tested. In addition, we did not detect a cell surface pool of endogenous GPI-linked proteins in caveolin-1 deficient fibroblasts—in contrast to the work of Nichols and colleagues, who used an exogenous GPI-anchored protein (63). This may be due to their use of a transient overexpression system rather than the study of endogenous GPI-linked proteins (this report). As we show that the uptake of cholera toxin (which binds to the glycolipid-GM1) is blocked in caveolin-1-deficient cells, it is highly unlikely that GPI-linked proteins (which are also tethered through a glycolipid linkage) are being rapidly endocytosed in our cell system. In addition, we and others have previously shown that the endocytosis of endogenous GPI-linked proteins (such as decay-accelerating factor [DAF]) is an extremely slow and inefficient process (see Fig. 4A in reference 45). Similarly, Nichols and colleagues concluded that the rate of transfer of GPI-green fluorescent protein from the Golgi to the plasma membrane (exocytosis) was ~22 times faster than the rate of transfer from the plasma membrane to the Golgi (endocytosis); as such, they calculated an average residence time of ~200 min at the plasma membrane and an average residence time of ~9 min within the Golgi complex. Thus, their data fit well with the notion of a Golgi-retention-driven pathway in caveolin-deficient cells that is dependent on the expression of palmitoylated caveolins.

ACKNOWLEDGMENTS

This work was supported by grants from the NIH, the Muscular Dystrophy Association (MDA), the Susan G. Komen Breast Cancer Foundation, and the American Heart Association (AHA), as well as a Hirschl/Weil-Caulier Career Scientist Award (all to M.P.L.). F.S. was a recipient of a fellowship from Telethon-Italia.

REFERENCES

1. **Ahmed, S. N., D. A. Brown, and E. London.** 1997. On the origin of sphingolipid/cholesterol-rich detergent-insoluble cell membranes: physiological concentrations of cholesterol and sphingolipid induce formation of a detergent-insoluble, liquid-ordered lipid phase in model membranes. Biochemistry **36:**10944–10953.
2. **Angst, B. D., C. Marcozzi, and A. Magee.** 2001. The cadherin superfamily: diversity in form and function. J. Cell Sci. **114:**629–641.
3. **Badizadegan, K., B. L. Dickinson, H. E. Wheeler, R. S. Blumberg, R. K. Holmes, and W. I. Lencer.** 2000. Heterogeneity of detergent-insoluble membranes from human intestine containing caveolin-1 and ganglioside G(M1). Am. J. Physiol. Gastroint. Liver Physiol. **278:**G895-G904.
4. **Bamezai, A., and K. L. Rock.** 1991. Effect of ras-activation on the expression of GPI-anchored proteins on the plasma membrane. Oncogene **6:**1445–1451.
5. **Brodsky, R. A., G. L. Mukhina, K. L. Nelson, T. S. Lawrence, R. J. Jones, and J. T. Buckley.** 1999. Resistance of paroxysmal nocturnal hemoglobinuria cells to the glycosylphosphatidylinositol-binding toxin aerolysin. Blood **93:**1749–1756.
6. **Brown, D., and J. K. Rose.** 1992. Sorting of GPI-anchored proteins to glycolipid-enriched membrane subdomains during transport to the apical cell surface. Cell **68:**533–544.
7. **Brown, D. A., B. Crise, and J. K. Rose.** 1989. Mechanism of membrane anchoring affects polarized expression of two proteins in MDCK cells. Science **245:**1499–1501.
8. **Brown, D. A., and E. London.** 1998. Functions of lipid rafts in biological membranes. Annu. Rev. Cell Dev. Biol. **14:**111–136.
9. **Brown, D. A., and E. London.** 1997. Structure of detergent-resistant membrane domains: does phase separation occur in biological membranes? Biochem. Biophys. Res. Commun. **240:**1–7.
10. **Buss, J. E., M. P. Kamps, K. Gould, and B. M. Sefton.** 1986. The absence of myristic acid decreases membrane binding of p60src but does not affect tyrosine protein kinase activity. J. Virol. **58:**468–474.
11. **Caras, I. W., G. N. Weddell, M. A. Davitz, V. Nussenzweig, and D. W. Martin, Jr.** 1987. Signal for attachment of a phospholipid membrane anchor in decay acelerating factor. Science **238:**1280–1283.
12. **Caras, J. W., G. N. Weddell, and S. R. Williams.** 1989. Analysis of the signal for attachment of a glycophospholipid membrane anchor. J. Cell Biol. **108:**1387–1396.
13. **Cavallone, D., N. Malagolini, and F. Serafini-Cessi.** 2001. Mechanism of release of urinary Tamm-Horsfall glycoprotein from the kidney GPI-anchored counterpart. Biochem. Biophys. Res. Commun. **280:**110–114.
14. **Couet, J., S. Li, T. Okamoto, P. S. Scherer, and M. P. Lisanti.** 1997. Molecular and cellular biology of caveolae: paradoxes and plasticities. Trends Cardiovasc. Med. **7:**103–110.
15. **Das, K., R. Y. Lewis, P. E. Scherer, and M. P. Lisanti.** 1999. The membrane spanning domains of caveolins 1 and 2 mediate the formation of caveolin hetero-oligomers. Implications for the assembly of caveolae membranes *in vivo*. J. Biol. Chem. **274:**18721–18728.
16. **Diep, D. B., K. L. Nelson, S. M. Raja, E. N. Pleshak, and J. T. Buckley.** 1998. Glycosylphosphatidylinositol anchors of membrane glycoproteins are binding determinants for the channel-forming toxin aerolysin. J. Biol. Chem. **273:**2355–2360.
17. **Dietzen, D. J., W. R. Hastings, and D. M. Lublin.** 1995. Caveolin is palmitoylated on multiple cysteine residues: palmitoylation is not necessary for localization of caveolin to caveolae. J. Biol. Chem. **270:**6838–6842.
18. **Drab, M., P. Verkade, M. Elger, M. Kasper, M. Lohn, B. Lauterbach, J. Menne, C. Lindschau, F. Mende, F. C. Luft, A. Schedl, H. Haller, and T. V. Kurzchalia.** 2001. Loss of caveolae, vascular dysfunction, and pulmonary defects in caveolin-1 gene-disrupted mice. Science **293:**2449–2452.

19. **Dupree, P., R. G. Parton, G. Raposo, T. V. Kurzchalia, and K. Simons.** 1993. Caveolae and sorting in the trans-Golgi network of epithelial cells. EMBO J. **12:**1597–1605.
20. **Engelman, J. A., C. C. Wycoff, S. Yasuhara, K. S. Song, T. Okamoto, and M. P. Lisanti.** 1997. Recombinant expression of caveolin-1 in oncogenically transformed cells abrogates anchorage-independent growth. J. Biol. Chem. **272:**16374–16381.
21. **Engelman, J. A., X. L. Zhang, F. Galbiati, D. Volonte, F. Sotgia, R. G. Pestell, C. Minetti, P. E. Scherer, T. Okamoto, and M. P. Lisanti.** 1998. Molecular genetics of the caveolin gene family: implications for human cancers, diabetes, Alzheimer's disease, and muscular dystrophy. Am. J. Hum. Genet. **63:** 1578–1587.
22. **Engelman, J. A., X. L. Zhang, B. Razani, P. R. G., and M. P. Lisanti.** 1999. p42/44 MAP kinase -dependent and -independent signaling pathways regulate caveolin-1 gene expression. Activation of Ras-MAP kinase and PKA signaling cascades transcriptionally down-regulates caveolin-1 promoter activity. J. Biol. Chem. **274:**32333–32341.
23. **Ferguson, M. A. J.** 1994. What can GPI do for you. Parasitol. Today **10:**48–52.
24. **Fleming, R. E., E. C. Crouch, C. A. Ruzicka, and W. S. Sly.** 1993. Pulmonary carbonic anhydrase IV: developmental regulation and cell-specific expression in the capillary endothelium. Am. J. Physiol. **265:**L627-L635.
25. **Fra, A. M., M. Masserini, P. Palestini, S. Sonnino, and K. Simons.** 1995. A photo-reactive derivative of ganglioside GM1 specifically cross-links VIP21-caveolin on the cell surface. FEBS Lett. **375:**11–14.
26. **Fra, A. M., E. Williamson, K. Simons, and R. G. Parton.** 1995. De novo formation of caveolae in lymphocytes by expression of VIP21-caveolin. Proc. Natl. Acad. Sci. USA **92:**8655–8659.
27. **Fra, A. M., E. Williamson, K. Simons, and R. G. Parton.** 1994. Detergent-insoluble glycolipid microdomains in lymphocytes in the absence of caveolae. J. Biol. Chem. **269:**30745–30748.
28. **Galbiati, F., J. A. Engelman, D. Volonte, X. L. Zhang, C. Minetti, M. Li, H. J. Hou, B. Kneitz, W. Edelmann, and M. P. Lisanti.** 2001. Caveolin-3 null mice show a loss of caveolae, changes in the microdomain distribution of the dystrophin-glycoprotein complex, and T-tubule abnormalities. J. Biol. Chem. **276:**21425–21433.
29. **Galbiati, F., B. Razani, and M. P. Lisanti.** 2001. Emerging themes in lipid rafts and caveolae. Cell **106:**403–411.
30. **Galbiati, F., B. Razani, and M. P. Lisanti.** 2001. Caveolae and caveolin-3 in muscular dystrophy. Trends Mol. Med. **7:**435–441.
31. **Gkantiragas, I., B. Brugger, E. Stuven, D. Kaloyanova, X. Y. Li, K. Lohr, F. Lottspeich, F. T. Wieland, and J. B. Helms.** 2001. Sphingomyelin-enriched microdomains at the Golgi Complex. Mol. Biol. Cell. **12:**1819–1833.
32. **Hagiwara, Y., T. Sasaoka, K. Araishi, M. Imamura, H. Yorifuji, I. Nonaka, E. Ozawa, and T. Kikuchi.** 2000. Caveolin-3 deficiency causes muscle degeneration in mice. Hum. Mol. Genet. **9:**3047–3054.
33. **Harris, J. S., D. E. Epps, S. R. Davio, and F. J. Kezdy.** 1995. Evidence for transbilayer, tail-to-tail cholesterol dimers in dipalmitoylglycerophosphocholine liposomes. Biochemistry **34:**3851–3857.
34. **Henley, J. R., E. W. Krueger, B. J. Oswald, and M. A. McNiven.** 1998. Dynamin-mediated internalization of caveolae. J. Cell Biol. **141:**85–99.
35. **Ivanyi, D., J. Janssen, and J. G. Collard.** 1986. Expression of Ly-6 and Thy-1 antigens on NIH 3T3 cells suppressed after transformation with activated human ras-oncogenes. Int. J. Cancer **38:**575–580.
36. **Koleske, A. J., D. Baltimore, and M. P. Lisanti.** 1995. Reduction of caveolin and caveolae in oncogenically transformed cells. Proc. Natl. Acad. Sci. USA **92:**1381–1385.
37. **Kurzchalia, T., P. Dupree, R. G. Parton, R. Kellner, H. Virta, M. Lehnert, and K. Simons.** 1992. VIP 21, A 21-kD membrane protein is an integral component of trans-Golgi-network-derived transport vesicles. J. Cell Biol. **118:**1003–1014.
38. **Lee, H., D. Volonte, F. Galbiati, P. Iyengar, D. M. Lublin, D. B. Bregman, M. T. Wilson, R. Campos-Gonzalez, B. Bouzahzah, R. G. Pestell, P. E. Scherer, and M. P. Lisanti.** 2000. Constitutive and growth factor-regulated phosphorylation of caveolin-1 occurs at the same site (Tyr-14) in vivo: identification of a c-Src/Cav-1/Grb7 signaling cassette. Mol. Endocrinol. **14:**1750–1775.
39. **Lee, H., S. E. Woodman, J. A. Engelman, D. Volonte', F. Galbiati, H. L. Kaufman, D. M. Lublin, and M. P. Lisanti.** 2001. Palmitoylation of caveolin-1 at a single site (Cys-156) controls its coupling to the c-Src tyrosine kinase. J. Biol. Chem. **276:**35150–35158.
40. **Li, S., J. Couet, and M. P. Lisanti.** 1996. Src tyrosine kinases, G alpha subunits and H-Ras share a common membrane-anchored scaffolding protein, Caveolin. Caveolin binding negatively regulates the auto-activation of Src tyrosine kinases. J. Biol. Chem. **271:**29182–29190.
41. **Li, S., F. Galbiati, D. Volonte, M. Sargiacomo, J. A. Engelman, K. Das, P. E. Scherer, and M. P. Lisanti.** 1998. Mutational analysis of caveolin-induced vesicle formation. Expression of caveolin-1 recruits caveolin-2 to caveolae membranes. FEBS Lett. **434:**127–134.
42. **Li, S., K. S. Song, S. S. Koh, A. Kikuchi, and M. P. Lisanti.** 1996. Baculovirus-based expression of mammalian caveolin in Sf21 insect cells. A model system for the biochemical and morphological study of caveolar biogenesis. J. Biol. Chem. **271:**28647–28654.
43. **Li, S., K. S. Song, and M. P. Lisanti.** 1996. Expression and characterization of recombinant caveolin: purification by poly-histidine tagging and cholesterol-dependent incorporation into defined lipid membranes. J. Biol. Chem. **271:**568–573.
44. **Lisanti, M. P., I. W. Caras, M. A. Davitz, and E. Rodriguez-Boulan.** 1989. A glycophospholipid membrane anchor acts as an apical targeting signal in polarized epithelial cells. J. Cell Biol. **109:**2145–2156.
45. **Lisanti, M. P., I. W. Caras, T. Gilbert, D. Hanzel, and E. Rodriguez-Boulan.** 1990. Vectorial apical delivery and slow endocytosis of a glycolipid-anchored fusion protein in transfected MDCK cells. Proc. Natl. Acad. Sci. USA **87:** 7419–7423.
46. **Lisanti, M. P., M. C. Field, I. W. Caras, A. K. Menon, and E. Rodriguez-Boulan.** 1991. Mannosamine, a novel inhibitor of glycosyl-phosphatidylinositol incorporation into proteins. EMBO J. **10:**1969–1977.
47. **Lisanti, M. P., A. Le Bivic, A. R. Saltiel, and E. Rodriguez-Boulan.** 1990. Prefered apical distribution of glycosyl-phosphatidylinositol (GPI) anchored proteins: a highly conserved feature of the polarized epithelial cell phenotype. J. Membr. Biol. **113:**155–167.
48. **Lisanti, M. P., A. Le Bivic, M. Sargiacomo, and E. Rodriguez-Boulan.** 1989. Steady-state distribution and biogenesis of endogenous MDCK glycoproteins: evidence for intracellular sorting and polarized cell surface delivery. J. Cell Biol. **109:**2117–2127.
49. **Lisanti, M. P., and E. Rodriguez-Boulan.** 1990. Glycophospholipid membrane anchoring provides clues to the mechanism of protein sorting in polarized epithelial cells. Trends Biochem. Sci. **15:**113–118.
50. **Lisanti, M. P., E. Rodriguez-Boulan, and A. R. Saltiel.** 1990. Emerging functional roles for the glycosyl-phosphatidylinositol (GPI) membrane protein anchor. J. Membr. Biol. **117:**1–10.
51. **Lisanti, M. P., M. Sargiacomo, L. Graeve, A. R. Saltiel, and E. Rodriguez-Boulan.** 1988. Polarized apical distribution of glycosyl-phosphatidylinositol anchored proteins in a renal epithelial cell line. Proc. Natl. Acad. Sci. USA **85:**9557–9561.
52. **Lisanti, M. P., P. Scherer, Z.-L. Tang, and M. Sargiacomo.** 1994. Caveolae, caveolin and caveolin-rich membrane domains: a signalling hypothesis. Trends Cell Biol. **4:**231–235.
53. **Lisanti, M. P., P. E. Scherer, J. Vidugiriene, Z.-L. Tang, A. Hermanoski-Vosatka, Y.-H. Tu, R. F. Cook, and M. Sargiacomo.** 1994. Characterization of caveolin-rich membrane domains isolated from an endothelial-rich source: Implications for human disease. J. Cell Biol. **126:**111–126.
54. **Lisanti, M. P., Z.-L. Tang, and M. Sargiacomo.** 1993. Caveolin forms a hetero-oligomeric protein complex that interacts with an apical GPI-linked protein: implications for the biogenesis of caveolae. J. Cell Biol. **123:**595–604.
55. **Lisanti, M. P., Z.-T. Tang, P. Scherer, and M. Sargiacomo.** 1995. Caveolae purification and GPI-linked protein sorting in polarized epithelia. Methods Enzymol. **250:**655–668.
56. **Monier, S., D. J. Dietzen, W. R. Hastings, D. M. Lublin, and T. V. Kurzchalia.** 1996. Oligomerization of VIP21-caveolin in vitro is stabilized by long chain fatty acylation or cholesterol. FEBS Lett. **388:**143–149.
57. **Monier, S., R. G. Parton, F. Vogel, J. Behlke, A. Henske, and T. Kurzchalia.** 1995. VIP21-caveolin, a membrane protein constituent of the caveolar coat, oligomerizes in vivo and in vitro. Mol. Biol. Cell **6:**911–927.
58. **Montesano, R., J. Roth, A. Robert, and L. Orci.** 1982. Non-coated membrane invaginations are involved in binding and internalization of cholera and tetanus toxins. Nature (London) **296:**651–653.
59. **Mora, R., V. Bonilha, A. Marmostein, P. E. Scherer, D. Brown, M. P. Lisanti, and E. Rodriguez-Boulan.** 1999. Caveolin-2 localizes to the Golgi complex but redistributes to plasma membrane, caveolae, and rafts when co-expressed with caveolin-1. J. Biol. Chem. **274:**25708–25717.
60. **Moran, P., H. Raab, W. J. Kohr, and I. W. Caras.** 1991. Glycophospholipid membrane anchor attachment: molecular analysis of the cleavage/attachment site. J. Biol. Chem. **266:**1250–1257.
61. **Murata, M., J. Peranen, R. Schreiner, F. Weiland, T. Kurzchalia, and K. Simons.** 1995. VIP21/caveolin is a cholesterol-binding protein. Proc. Natl. Acad. Sci. USA **92:**10339–10343.
62. **Nelson, K. L., S. M. Raja, and J. T. Buckley.** 1997. The glycosylphosphatidylinositol-anchored surface glycoprotein Thy-1 is a receptor for the channel-forming toxin aerolysin. J. Biol. Chem. **272:**12170–12174.
63. **Nichols, B. J., A. K. Kenworthy, R. S. Polishchuk, R. Lodge, T. H. Roberts, K. Hirschberg, R. D. Phair, and J. Lippincott-Schwartz.** 2001. Rapid cycling of lipid raft markers between the cell surface and Golgi complex. J. Cell Biol. **153:**529–541.
64. **Oh, P., D. P. McIntosh, and J. E. Schnitzer.** 1998. Dynamin at the neck of caveolae mediates their budding to form transport vesicles by GTP-driven fission from the plasma membrane of endothelium. J. Cell Biol. **141:**101–114.
65. **Orlandi, P. A., and P. H. Fishman.** 1998. Filipin-dependent inhibition of cholera toxin: evidence for toxin internalization and activation through caveolae-like domains. J. Cell Biol. **141:**905–915.
66. **Palade, G. E., and R. R. Bruns.** 1968. Structural modification of plasmalemmal vesicles. J. Cell Biol. **37:**633–649.
67. **Parolini, I., M. Sargiacomo, F. Galbiati, G. Rizzo, F. Grignani, J. A. En-**

gelman, T. Okamoto, T. Ikezu, P. E. Scherer, R. Mora, E. Rodriguez-Boulan, C. Peschle, and M. P. Lisanti. 1999. Expression of caveolin-1 is required for the transport of caveolin-2 to the plasma membrane. J. Biol. Chem. **274:** 25718–25725.

68. **Parolini, I., M. Sargiacomo, M. P. Lisanti, and C. Peschle.** 1996. Signal transduction and GPI-linked proteins (Lyn, Lck, CD4, CD45, G proteins, CD 55) selectively localize in Triton-insoluble plasma membrane domains of human leukemic cell lines and normal granulocytes. Blood **87:**3783–3794.
69. **Parton, R. G.** 1994. Ultrastructural localization of gangliosides: GM1 is concentrated in caveolae. J. Histochem. Cytochem. **42:**155–166.
70. **Parton, R. G., M. Way, N. Zorzi, and E. Stang.** 1997. Caveolin-3 associates with developing T-tubules during muscle differentiation. J. Cell Biol. **136:**137–154.
71. **Philippova, M. P., V. N. Bochkov, D. V. Stambolsky, V. A. Tkachuk, and T. J. Resink.** 1998. T-cadherin and signal-transducing molecules co-localize in caveolin-rich membrane domains of vascular smooth muscle cells. FEBS Lett. **429:**207–210.
72. **Razani, B., J. A. Engelman, X. B. Wang, W. Schubert, X. L. Zhang, C. B. Marks, F. Macaluso, R. G. Russell, M. Li, R. G. Pestell, D. Di Vizio, H. J. Hou, B. Kneitz, G. Lagaud, G. J. Christ, W. Edelmann, and M. P. Lisanti.** 2001. Caveolin-1 null mice are viable but show evidence of hyperproliferative and vascular abnormalities. J. Biol. Chem. **276:**38121–38138.
73. **Razani, B., and M. P. Lisanti.** 2001. Caveolin-deficient mice: insights into caveolar function and human disease. J. Clin. Investig. **108:**1553–1561.
74. **Rindler, M. J., S. S. Naik, N. Li, T. C. Hoops, and M. N. Peraldi.** 1990. Uromodulin (Tamm-Horsfall glycoprotein/uromucoid) is a phosphatidylinositol-linked membrane protein. J. Biol. Chem. **265:**20784–20789.
75. **Rothberg, K. G., J. E. Heuser, W. C. Donzell, Y. Ying, J. R. Glenney, and R. G. W. Anderson.** 1992. Caveolin, a protein component of caveolae membrane coats. Cell **68:**673–682.
76. **Sargiacomo, M., M. P. Lisanti, L. Graeve, A. LeBivic, and E. Rodriguez-Boulan.** 1989. Integral and peripheral protein composition of the apical and basolateral membrane domains in MDCK cells. J. Membr. Biol. **107:**277–286.
77. **Sargiacomo, M., P. E. Scherer, Z.-L. Tang, E. Kubler, K. S. Song, M. C. Sanders, and M. P. Lisanti.** 1995. Oligomeric structure of caveolin: implications for caveolae membrane organization. Proc. Natl. Acad. Sci. USA **92:**9407–9411.
78. **Sargiacomo, M., M. Sudol, Z.-L. Tang, and M. P. Lisanti.** 1993. Signal transducing molecules and GPI-linked proteins form a caveolin-rich insoluble complex in MDCK cells. J. Cell Biol. **122:**789–807.
79. **Scheiffele, P., P. Verkade, A. M. Fra, H. Virta, K. Simons, and E. Ikonen.** 1998. Caveolin-1 and -2 in the exocytic pathway of MDCK cells. J. Cell Biol. **140:**795–806.
80. **Scherer, P. E., G. Z. Lederkremer, S. Williams, M. Fogliano, G. Baldini, and H. F. Lodish.** 1996. Cab45, a novel (Ca2+)-binding protein localized to the Golgi lumen. J. Cell Biol. **133:**257–268.
81. **Scherer, P. E., R. Y. Lewis, D. Volonte, J. A. Engelman, F. Galbiati, J. Couet, D. S. Kohtz, E. van Donselaar, P. Peters, and M. P. Lisanti.** 1997. Cell-type and tissue-specific expression of caveolin-2. Caveolins 1 and 2 co-localize and form a stable hetero-oligomeric complex *in vivo*. J. Biol. Chem. **272:**29337–29346.
82. **Scherer, P. E., T. Okamoto, M. Chun, I. Nishimoto, H. F. Lodish, and M. P. Lisanti.** 1996. Identification, sequence and expression of caveolin-2 defines a caveolin gene family. Proc. Natl. Acad. Sci. USA **93:**131–135.
83. **Scherer, P. E., Z.-L. Tang, M. C. Chun, M. Sargiacomo, H. F. Lodish, and M. P. Lisanti.** 1995. Caveolin isoforms differ in their N-terminal protein sequence and subcellular distribution: identification and epitope mapping of an isoform-specific monoclonal antibody probe. J. Biol. Chem. **270:**16395–16401.
84. **Schubert, W., P. G. Frank, B. Razani, D. Park, C.-W. Chow, and M. P. Lisanti.** 2001. Caveolae-deficient endothelial cells show defects in the uptake and transport of albumin *in vivo*. J. Biol. Chem. **276:**48619–48622.
85. **Shogomori, H., and A. H. Futerman.** 2001. Cholera toxin is found in detergent-insoluble rafts/domains at the cell surface of hippocampal neurons but is internalized via a raft-independent mechanism. J. Biol. Chem. **276:**9182–9188.
86. **Simionescu, N.** 1983. Cellular aspects of transcapillary exchange. Physiol. Rev. **63:**1536–1560.
87. **Smart, E. J., G. A. Graf, M. A. McNiven, W. C. Sessa, J. A. Engelman, P. E. Scherer, T. Okamoto, and M. P. Lisanti.** 1999. Caveolins, liquid-ordered domains, and signal transduction. Mol. Cell. Biol. **19:**7289–7304.
88. **Song, K. S., M. Sargiacomo, F. Galbiati, M. Parenti, and M. P. Lisanti.** 1997. Targeting of a G alpha subunit (G_{i1} alpha) and c-Src tyrosine kinase to caveolae membranes: clarifying the role of N-myristoylation. Cell. Mol. Biol. (Noisy-Le-Grand) **43:**293–303.
89. **Song, K. S., P. E. Scherer, Z.-L. Tang, T. Okamoto, S. Li, M. Chafel, C. Chu, D. S. Kohtz, and M. P. Lisanti.** 1996. Expression of caveolin-3 in skeletal, cardiac, and smooth muscle cells. Caveolin-3 is a component of the sarcolemma and co-fractionates with dystrophin and dystrophin-associated glycoproteins. J. Biol. Chem. **271:**15160–15165.
90. **Song, K. S., Z.-L. Tang, S. Li, and M. P. Lisanti.** 1997. Mutational analysis of the properties of caveolin-1. A novel role for the C-terminal domain in mediating homotypic caveolin-caveolin interactions. J. Biol. Chem. **272:**4398–4403.
91. **Soole, K. L., M. A. Jepson, G. P. Hazlewood, H. J. Gilbert, and B. H. Hirst.** 1995. Epithelial sorting of a glycosylphosphatidylinositol-anchored bacterial protein expressed in polarized renal MDCK and intestinal Caco-2 cells. J. Cell Sci. **108:**369–377.
92. **Tang, Z.-L., P. E. Scherer, T. Okamoto, K. Song, C. Chu, D. S. Kohtz, I. Nishimoto, H. F. Lodish, and M. P. Lisanti.** 1996. Molecular cloning of caveolin-3, a novel member of the caveolin gene family expressed predominantly in muscle. J. Biol. Chem. **271:**2255–2261.
93. **Torgersen, M. L., G. Skretting, B. van Deurs, and K. Sandvig.** 2001. Internalization of cholera toxin by different endocytic mechanisms. J. Cell Sci. **114:**3737–3747.
94. **Uittenbogaard, A., and E. J. Smart.** 2000. Palmitoylation of caveolin-1 is required for cholesterol binding, chaperone complex formation, and rapid transport of cholesterol to caveolae. J. Biol. Chem. **275:**25595–25599.
95. **Yamada, E.** 1955. The fine structure of the gall bladder epithelium of the mouse. J. Biophys. Biochem. Cytol. **1:**445–458.